PB 211 897

A.R.A.P. REPORT NO. 169

AN INITIAL TEST OF THE APPLICABILITY OF INVARIANT MODELING METHODS TO ATMOSPHERIC BOUNDARY LAYER DIFFUSION

Coleman duP. Donaldson

and

Glenn R. Hilst

Reproduced by
NATIONAL TECHNICAL
INFORMATION SERVICE
U S Department of Commerce
Springfield VA 22151

October 1971

to

Environmental Protection Agency
National Environmental Research Center
Division of Meteorology
Research Triangle Park, North Carolina 27711

EPA Contract No. 68-02-0014

AERONAUTICAL RESEARCH ASSOCIATES OF PRINCETON, INC.
50 Washington Road, Princeton, New Jersey 08540

147

BIBLIOGRAPHIC DATA SHEET	1. Report No. APTD-1149	2.	3. Recipient's Accession No.

4. Title and Subtitle
An Initial Test of the Applicability of Invariant Modeling Methods to Atmospheric Boundary Layer Diffusion

5. Report Date
October 1971

6.

7. Author(s)
Coleman duP. Donaldson and Glenn R. Hilst

8. Performing Organization Rept. No. A.R.A.P. No. 169

9. Performing Organization Name and Address
AERONAUTICAL RESEARCH ASSOCIATES OF PRINCETON, INC.
50 Washington Road
Princeton, New Jersey 08540

10. Project/Task/Work Unit No.

11. Contract/Grant No.
68-02-0014

12. Sponsoring Organization Name and Address
ENVIRONMENTAL PROTECTION AGENCY
National Environmental Research Center
Division of Meteorology
Research Triangle Park, North Carolina 27711

13. Type of Report & Period Covered

14.

15. Supplementary Notes

16. Abstracts As a first assembly of the principles and methods of invariant modeling for the simulation of turbulent diffusion in the atmospheric boundary layer, the results were considered successful beyond reasonable expectation. With only prior knowledge of the mean wind and temperature profiles and using a relationship between the macroscale and the dissipation scale derived for laboratory scale flow, the structure of turbulence and the diffusion of matter are simulated well within an order of magnitude of observed values. In most cases, the verification is within a factor of two, a result which has been achieved for other modeling techniques only after much more effort and resort to empiricism. Perhaps most importantly at this stage of development of the invariant model, all of the classical requirements for asymptotic behavior of the diffusion are met. The predictions were somewhat more exact for neutral and unstable temperature stratification than for stably stratified atmospheres, but even the latter were remarkable considering the general lack of any satisfactory theory for diffusion in stably stratified atmospheres. A greater understanding of the physics of turbulent transport has been achieved and has led directly to further improvement and refinement of the model. The dependence of the scale on stability has been clarified and, although this dependence is not fully understood, it is clear that the ratio of the scale of the breadth of a pollutant plume to the integral scale of the velocity fluctuations in the atmosphere plays a very important role in the physics of the disposal process.

17. Key Words and Document Analysis. 17a. Descriptors

Air pollution
Mathematical models
Atmospheric diffusion
Wind (meteorology)
Temperature
Turbulence
Stability
Plumes

17b. Identifiers/Open-Ended Terms

17c. COSATI Field/Group 13B

18. Availability Statement
Unlimited

19. Security Class (This Report) UNCLASSIFIED

21. No. of Pages 65

20. Security Class (This Page UNCLASSIFIED

22. Price $3.00

TABLE OF CONTENTS

		Page No.
	Nomenclature	iii
1.	Introduction	1
2.	The Basic Diffusion Equations and Method of Closure	4
	2.1 Closure at Higher-Order Moments	7
	2.2 The Method of Closure at Second-Order Moments	8
3.	The Invariant Diffusion Model	12
4.	Some Relationships Between Second-Order and First-Order Closure Models	18
	4.1 K_m^* from First- and Second-Order Closure Models in a Neutrally Stratified, Constant Shear Stress Layer	22
5.	Initial Tests of the Model	26
	5.1 An Example	27
	5.2 An Initial Test of the Effect of Stability	29
	5.3 The Sensitivity of Diffusion to the Scale Length	31
6.	A Calculation of the Time Required for Turbulence to Become Fully Developed	35
7.	Conclusions	37
8.	References	39
	Figures 1 through 12	40
	Appendix A	52

Nomenclature

a, b	constants
C, C_p	pollutant concentration (mass fraction)
c	specific heat at constant pressure
g	acceleration of gravity
i	subscript index
K	$\overline{u'^2} + \overline{v'^2} + \overline{w'^2}$
K_H^*, K_m^*, K_y^*, K_z^*	eddy diffusivities for heat, momentum, and matter
k	von Kármán's constant
L	Monin-Obukhov length
n	an integer, 1, 2, 3,...
p	pressure
Re_Λ	turbulent Reynolds number
R_i	Richardson number
S	source or sink strength of pollutant (per unit volume and time)
$\bar{T}$, T'	mean and fluctuating values of potential temperature
t	time
$\bar{u}$, $\bar{v}$, $\bar{w}$	time-averaged components of fluid motion
u', v', w'	turbulent components of fluid motion
x, y, z	Cartesian coordinate system
$\mathscr{D}$	molecular diffusivity
α, β	Monin-Obukhov coefficients
Λ, λ	diffusivity and dissipation scale lengths
μ_o	viscosity
μ_2	second viscosity coefficient
ρ, ρ_o	fluid density

An overbar indicates a time-averaged value of the quantity; a prime indicates an instantaneous fluctuation of that quantity about its average value. Averages of products of fluctuations of two or more quantities are sometimes referred to as correlation terms.

$\partial/\partial t$	local time derivative
$\partial/\partial x_i$	local space derivative

$$\frac{d}{dt} \doteq \frac{\partial}{\partial t} + u\frac{\partial}{\partial x} + v\frac{\partial}{\partial y} + w\frac{\partial}{\partial z}$$

1. INTRODUCTION

Recent emphases on the alleviation and prevention of significant air pollution problems have placed a new premium on reliable methods for predicting the transport, diffusion, chemical reaction, and deposition of airborne materials emanating from man-made sources. Since the capacity of the lower atmosphere to disperse airborne wastes to harmless concentrations varies through two or more orders of magnitude within a single day and from one place to another, this variable alone determines to a large extent the feasible utilization of the atmosphere for waste disposal.

A variety of techniques for predicting atmospheric dispersion have been brought forward to address this waste management problem. These techniques vary in sophistication from simple kinematic descriptions of the accumulation of pollutants within a hypothetically closed box to highly complicated computer solutions of the combined equations of atmospheric motion and complex photochemical chain reactions. At the present stage of development, all of these models require a large content of empirical knowledge, a feature which makes their application to new meteorological conditions, different terrain, or new pollutant source geometries highly questionable.

The work reported here represents an initial attempt to remove some of this empiricism from atmospheric diffusion calculations by an appeal to a more rigorous physical description of the process of turbulent diffusion in the lower atmosphere. In particular, it has appeared worthwhile to investigate the applicability of the method of invariant modeling of turbulent fluid flows to the lower atmosphere and its diffusion capabilities. These techniques, which have been successfully applied to classical shear flows (such as the free jet, the plane shear layer, and the free vortex) depend upon

a closure of the governing equations at the level of the equations for the second-order correlations or moments of turbulent fluctuations. These moments contain, among others, the correlations responsible for the transport of momentum, heat, and matter by the turbulent motion. The success of these techniques in predicting the structure of turbulence in classical shear flows with rather a wide variety of geometries, e.g., from free jet to free vortex, suggested that the modeling might be profitably carried over to the more complicated atmospheric flows and the turbulent diffusion of a pollutant.

Discussions of this possibility with the Division of Meteorology of the Environmental Protection Agency led to the conclusion that a test of the invariant modeling technique, in its simplest form, should precede any further significant development of these concepts for atmospheric problems. It was, therefore, agreed that a modest effort to test the model for the case of an infinite cross-wind line source in the lower atmosphere would be undertaken as a first demonstration of the general utility of this technique. Successful demonstration of the model for relatively simple source and atmospheric flow conditions would presumably justify additional refinement and development of the technique. In particular, the ability of the method to provide more precise physical insights into the complicated mechanisms of turbulent diffusion in arbitrarily stratified atmospheres was to be pursued at a later stage.

The initial tests of the earliest model have been completed and are reported here. These have been successful beyond reasonable expectations. In particular, using only the mean wind and temperature profiles for the lower atmosphere and a predetermined scale length, the vertical dispersion of a pollutant has been predicted well within a factor of two of observed values out to distances of about two miles. The predictions were somewhat more exact for neutral and unstable temperature stratification than for stably stratified atmospheres, but even the latter were remarkable considering the

general lack of any satisfactory theory for diffusion instably stratified atmospheres.

Even with these successes, the present effort has been most instructive. A greater understanding of the physics of turbulent transport has been achieved and has led directly to further improvement and refinement of the model. The dependence of the scale on stability has been clarified and, although this dependence is not fully understood, it is clear that the ratio of the scale of the breadth of a pollutant plume to the integral scale of the velocity fluctuations in the atmosphere plays a very important role in the physics of the dispersal process.

With the successful demonstration of this primitive form of the invariant model, attention has been turned to the refinement of the model in the light of recent numerical studies of classical shear flow, the construction of a three-dimensional diffusion model, and the application of these results to initial calculations of diffusion in arbitrarily stratified atmospheres. Among the refinements planned is the inclusion of the coriolis forces in the equations of motion so that diffusive effects within the Ekman layer may be calculated.

2. THE BASIC DIFFUSION EQUATIONS AND METHOD OF CLOSURE

Since the advent of the Navier-Stokes equations and Reynolds' introduction into these equations of the mean and fluctuating components of the vector and scalar quantities involved, various attempts have been made to construct predictive models for the structure and diffusive characteristics of turbulent fluid flows. The unclosed character of these equations and the lack of powerful computers has, until recently, dictated the use of only the very simplest schemes for a modeling closure of the equations of motion. These methods were not without merit and fruitful results; to the contrary, much of our present engineering competence in areas such as fluid flow in pipes, boundary layer flow, and even atmospheric diffusion processes has depended heavily upon these early insights and the organized empiricism to which they gave rise.

Although it is not our intention to review the development of methods for computing turbulent shear flow (the reader interested in such a review should consult Reference 1), it is instructive to recapitulate the most frequently used method for closure of the governing equations as background to the present method of closure developed by Donaldson and termed, "invariant modeling." The earlier methods of closure are readily illustrated by manipulation of the differential equation for the passive dispersion of matter in an incompressible fluid undergoing turbulent motion.

Let C be the mass fraction of a suspended gas or aerosol, ρ the density of the fluid, and let us adopt a cartesian coordinate system (x,y,z) with the components of fluid flow u, v, w along each of these directions. Then the governing equation for C, following the motion of a tagged fluid element, is

$$\rho \frac{dC}{dt} = \rho \frac{\partial C}{\partial t} + \rho u \frac{\partial C}{\partial x} + \rho v \frac{\partial C}{\partial y} + \rho w \frac{\partial C}{\partial z}$$

$$= \frac{\partial}{\partial x}\left(\rho \mathcal{D} \frac{\partial C}{\partial x}\right) + \frac{\partial}{\partial y}\left(\rho \mathcal{D} \frac{\partial C}{\partial y}\right) + \frac{\partial}{\partial z}\left(\rho \mathcal{D} \frac{\partial C}{\partial z}\right) + S \qquad (1)$$

where $\mathcal{D}$ is the molecular diffusivity and S is any local source or sink. Following Reynolds, we now separate the variables u, v, w, and C into their mean and fluctuating parts, i.e., $u = \bar{u} + u'$, $v = \bar{v} + v'$, $w = \bar{w} + w'$, and $C = \bar{C} + C'$. When these identities are substituted into Eq. (1) and use is made of the fact that, for incompressible flow,

$$\frac{\partial u'}{\partial x} + \frac{\partial v'}{\partial y} + \frac{\partial w'}{\partial z} = 0 \qquad (2)$$

Eq. (1) may, after being time-averaged, be written

$$\rho \frac{\partial \bar{C}}{\partial t} + \rho \bar{u} \frac{\partial \bar{C}}{\partial x} + \rho \bar{v} \frac{\partial \bar{C}}{\partial y} + \rho \bar{w} \frac{\partial \bar{C}}{\partial z} =$$

$$\frac{\partial}{\partial x}\left(\rho \mathcal{D} \frac{\partial \bar{C}}{\partial x} - \rho \overline{u'C'}\right) + \frac{\partial}{\partial y}\left(\rho \mathcal{D} \frac{\partial \bar{C}}{\partial y} - \rho \overline{v'C'}\right)$$

$$+ \frac{\partial}{\partial z}\left(\rho \mathcal{D} \frac{\partial \bar{C}}{\partial z} - \rho \overline{w'C'}\right) + \bar{S} \qquad (3)$$

For simplicity, we assume the mean motion to be steady with $\bar{v} = \bar{w} = 0$ and consider a steady point source of material C. Then downstream of the source, Eq. (3) may be written

$$\rho \bar{u} \frac{\partial \bar{C}}{\partial x} = \frac{\partial}{\partial x}\left(\rho \mathcal{D} \frac{\partial \bar{C}}{\partial x} - \rho \overline{u'C'}\right) + \frac{\partial}{\partial y}\left(\rho \mathcal{D} \frac{\partial \bar{C}}{\partial y} - \rho \overline{v'C'}\right)$$

$$+ \frac{\partial}{\partial z}\left(\rho \mathcal{D} \frac{\partial \bar{C}}{\partial z} - \rho \overline{w'C'}\right) \qquad (4)$$

The basic diffusion equation which it is customary to use is obtained from Eq. (4) by noting the experimental fact that gradients of mean quantities in directions normal to the mean motion are generally much larger than gradients in the direction of this motion, so that the term

$$\frac{\partial}{\partial x}\left(\rho\mathscr{D}\frac{\partial\overline{C}}{\partial x} - \rho\overline{u'C'}\right)$$

in (3) may be neglected. Under this assumption, which we shall adopt only for convenience since it is not required, the diffusion equation that one wishes to solve is

$$\rho\bar{u}\,\frac{\partial\overline{C}}{\partial x} = \frac{\partial}{\partial y}\left(\rho\mathscr{D}\frac{\partial\overline{C}}{\partial y} - \rho\overline{v'C'}\right) + \frac{\partial}{\partial z}\left(\rho\mathscr{D}\frac{\partial\overline{C}}{\partial z} - \rho\overline{w'C'}\right) \tag{5}$$

This equation may be solved, subject to appropriate initial and boundary conditions, if we specify some relation between the second-order correlations $\overline{C'v'}$ and $\overline{C'w'}$ and the mean distributions of concentration and velocity. Such a simple closure is useful, provided the flow is such that the dynamics of the second-order correlations can readily follow or "track" changes in the mean quantities.

Arguing from the physical rationale of a "mixing length" analogous to a molecular mean free path, Prandtl provided an early closure scheme by writing

$$\rho\overline{C'v'} = -\rho K_y^*\,\frac{\partial\overline{C}}{\partial y} \tag{6}$$

and

$$\rho\overline{C'w'} = -\rho K_z^*\,\frac{\partial\overline{C}}{\partial z} \tag{7}$$

where K_y^* and K_z^* are <u>eddy</u> diffusivities, quite analogous to but generally much larger than the molecular diffusivity $\mathscr{D}$. Substitution of Eqs. (6) and (7) into (5) yields the well-known diffusion equation

$$\rho\bar{u}\frac{\partial\overline{C}}{\partial x} = \frac{\partial}{\partial y}\left[\rho(\mathscr{D} + K_y^*)\frac{\partial\overline{C}}{\partial y}\right] + \frac{\partial}{\partial z}\left[\rho(\mathscr{D} + K_z^*)\frac{\partial\overline{C}}{\partial z}\right] \qquad (8)$$

Strictly speaking, Eqs. (6) and (7) only define K_y^* and K_z^* and closure is not achieved until these parameters are specified as a function of position and the fluid flow and concentration fields. A very large literature devoted to these specifications of eddy diffusivity continues to this day.

At the present, our concern is not with the successes or failures of this method of closure but, rather, with clear identification of the method itself. Stated generally, the principle involved is that <u>closure may be achieved by modeling the nth order correlations in terms of the lower order correlations</u>. Prandtl's method, which has just been described, invokes this principle at its lowest possible level, i.e., $n = 2$. Thus, the prevalent methods of closure retain only the minimum information inherent in the governing equations, since any effects of second- or higher-order moments are assumed to be explicitly contained in the mean values and the scale lengths of the flow and concentration fields. Since $n = 2$ is the minimum level at which closure may be obtained, we shall term methods such as Prandtl's "first-order closure."

2.1 Closure at Higher-Order Moments

Since, in principle, closure may be achieved at any order of correlation, the possibility of retaining significant information by closure at the third- or higher-order moments appears worth investigation. The techniques for deriving equations for the higher-order moments have been known for some time (for a complete derivation, see Reference 1, p. 250, et seq). To illustrate the technique, we note, for example,

$$\frac{\partial C'v'}{\partial t} = C' \frac{\partial v'}{\partial t} + v' \frac{\partial C'}{\partial t} \tag{9}$$

and

$$\frac{\partial v'}{\partial t} = \frac{\partial v}{\partial t} - \frac{\partial \bar{v}}{\partial t} \tag{10}$$

$$\frac{\partial C'}{\partial t} = \frac{\partial C}{\partial t} - \frac{\partial \bar{C}}{\partial t} \tag{11}$$

From the equation of motion for v and the diffusion equation for C, we form the mean values $\partial\bar{v}/\partial t$ and $\partial\bar{C}/\partial t$, subtract these from the original equations to find $\partial v'/\partial t$ and $\partial C'/\partial t$, and then multiply by C' and v', respectively, and add. We then take the time average of this equation to find $\partial\overline{C'v'}/\partial t$. When this process is carried out, we always find the resultant equation contains the next higher correlation or moment, e.g., $\overline{v'v'C'}$; hence, with each prediction equation for the nth correlation, we invoke a new unknown, the n+1 correlation term. Closure, therefore, depends upon successful modeling of the n+1 correlation terms in terms of the lower correlations for mean values of the flow field. It is to this problem that the methods of invariant modeling have been primarily addressed.

2.2 The Method of Closure at Second-Order Moments

Against the background considerations outlined above, we may note generally that any attempt to model turbulent fluid motions and the diffusion of a passive pollutant involves consideration of seven variables:

u, v, w	the components of fluid motion
T	the fluid temperature
p	the pressure
ρ	the fluid density
C	the concentration of pollutant

To construct a model we must have seven governing equations for these variables. These are supplied by the Navier-Stokes equations (three equations), the diffusion equations for heat and matter (two equations), the equation of mass continuity, and the equation of state. The latter equation relates p, T, and ρ and reduces the independent variables to six.

From these governing equations, we may develop the equations for any higher-order moments that we wish to consider. If we wish to attempt closure at the second-order moments, i.e., model any third-order moments in terms of second- and first-order moments, and we have six independent variables, we must, in general, develop equations for the following twenty-seven first- and second-order moments.

First-order moments:	
$\bar{u}$, $\bar{v}$, $\bar{w}$, $\bar{p}$, $\bar{T}$, $\bar{C}$	6 equations
Second-order moments:	
$\overline{u'^2}$, $\overline{v'^2}$, $\overline{w'^2}$, $\overline{T'^2}$, $\overline{p'^2}$, $\overline{C'^2}$	6
$\overline{u'v'}$, $\overline{v'w'}$, $\overline{u'w'}$	3
$\overline{u'T'}$, $\overline{v'T'}$, $\overline{w'T'}$	3
$\overline{u'p'}$, $\overline{v'p'}$, $\overline{w'p'}$, $\overline{p'T'}$	4
$\overline{u'C'}$, $\overline{v'C'}$, $\overline{w'C'}$, $\overline{C'T'}$, $\overline{C'p'}$	5
Total Equations	27

In principle, and given successful modeling of third-order moments in terms of lower order moments, we should be prepared to contend with 27 simultaneous partial differential equations, a prodigious task indeed.

Fortunately, the required equations are reduced significantly by several considerations. First, two of these moments do not appear in the derived moment equations, namely, $\overline{p'^2}$ and $\overline{C'^2}$. Equations may be written for these variances, but they do not feed back and are, therefore, not required for closure. Second, we may eliminate the following moments by assuming a

horizontal straight-line (nonconvergent) flow and an incompressible fluid:

$$\bar{v},\ \bar{w},\ \overline{v'v'},\ \overline{v'w'},\ \overline{w'w'}$$

a further reduction by five equations.

As a further step in reducing the number of equations, $\bar{p}$ has been eliminated by linearizing the equations, using essentially the Boussinesq approximation for small departures of p, T, and ρ from their values in an adiabatic atmosphere at rest. According to the methods of invariant modeling, the covariance of pressure fluctuation and each of the other five variables are modeled in terms of the remaining moments. This procedure which is described in the appendix removes $\overline{u'p'}$, $\overline{v'p'}$, $\overline{w'p'}$, $\overline{p'T'}$, and $\overline{p'C'}$ from separate consideration.

These considerations reduce the number of simultaneous partial differential equations from 27 to 14. In the early version of the invariant model, one more equation has been eliminated by retention of the assumption of a continuous pollutant source and that $\partial\overline{u'C'}/\partial x$ is negligible compared with $\partial\overline{v'C'}/\partial y$ and $\partial\overline{w'C'}/\partial z$ in this case. Under this assumption, the turbulence model developed from second-order closure involves 13 simultaneous partial differential equations for first- and second-order moments. In addition, this method of closure involves two scale lengths: the scale of the turbulence Λ which we treat as a free parameter, and the dissipation scale length λ which is related to Λ by an algebraic expression in terms of the components a and b, $u'^2 + v'^2 + w'^2 = K$, the fluid density ρ, and the molecular viscosity μ_o (see page 17).

In the general case of an active pollutant, e.g., a pollutant which is not without respect to the fluid temperature, the 13 partial differential equations must be solved simultaneously. However, for passive pollutants there is no feedback from the pollutant diffusion equations to the fluid

flow equations. Under this assumption, the equations for $\overline{C}$, $\overline{v'C'}$, $\overline{w'C'}$, and $\overline{C'T'}$ may be decoupled and solved separately after solutions for the remaining nine moments associated with the fluid flow and temperature have been obtained. In the early tests of the model reported here, a further economy of computer operation has been realized by taking known values of $\bar{u}(z)$ and $\overline{T}(z)$ as <u>fixed</u> inputs to the program. Under this mode of operation, the equations for $\bar{u}$ and $\overline{T}$ are not solved, reducing the number of simultaneous partial differential equations for the turbulence component of the model from 9 to 7.

Beyond the general considerations discussed above, the development of the invariant model for turbulence and diffusion has depended upon techniques for modeling third-order moments in terms of first- and second-order moments. The development of these techniques has been discussed by Donaldson and his colleagues [2, 3, 4, and 5] (Ref. 5 is appended to this report) and will not be repeated in detail here. (A more rigorous report of the development of these techniques and their application is now planned, following this successful initial test of the concepts involved.)

3. THE INVARIANT DIFFUSION MODEL

When the procedures of invariant modeling are systematically applied to the equations of motion for the atmospheric boundary layer and the diffusion equations for a (scalar) contaminant, the simplest set of simultaneous partial differential equations for the prediction of the diffusion of a contaminant emitted continuously from a point source is as follows:

1. The diffusion equation*

$$\rho_o \bar{u} \frac{\partial \overline{C}_p}{\partial x} = \overline{S} + \frac{\partial}{\partial y}\left(\mu_o \frac{\partial \overline{C}_p}{\partial y} - \rho_o \overline{C'_p v'}\right) + \frac{\partial}{\partial z}\left(\mu_o \frac{\partial \overline{C}_p}{\partial z} - \rho_o \overline{C'_p w'}\right) \tag{12}$$

This equation states that the rate of change of the average concentration $\overline{C}_p$, following the motion, is equal to any local source or sink plus the local diffusion due to molecular motions $\mu_o \partial^2 \overline{C}_p / \partial y^2$ and the local flux divergence $-\partial(\rho_o \overline{C'_p v'})/\partial y$. (We retain the molecular terms throughout this development so that the equations may be solved right down to the solid boundary.)

2. The turbulent flux equations

$$\begin{aligned}
\rho_o \bar{u} \frac{\partial \overline{C'_p v'}}{\partial x} = & -\rho_o \overline{v'v'} \frac{\partial \overline{C}_p}{\partial y} + 3 \frac{\partial}{\partial y}\left(\rho_o \Lambda \sqrt{K} \frac{\partial \overline{C'_p v'}}{\partial y}\right) \\
& + \frac{\partial}{\partial z}\left(\rho_o \Lambda \sqrt{K} \frac{\partial \overline{C'_p v'}}{\partial z}\right) + \frac{\partial}{\partial y}\left(\rho_o \Lambda \sqrt{K} \frac{\partial \overline{C'_p w'}}{\partial z}\right) \\
& + \frac{\partial}{\partial z}\left(\rho_o \Lambda \sqrt{K} \frac{\partial \overline{C'_p w'}}{\partial y}\right) - \frac{\rho_o \sqrt{K}}{\Lambda} \overline{C'v'} \\
& + \mu_o \left(\frac{\partial^2 \overline{C'_p v'}}{\partial y^2} + \frac{\partial^2 \overline{C'_p v'}}{\partial z^2} - \frac{2\overline{C'_p v'}}{\lambda^2}\right)
\end{aligned} \tag{13}$$

*This development is made under the assumption that the Schmidt number $\rho_o \mathscr{D}/\mu_o = 1$, or $\mu_o = \rho_o \mathscr{D}$, and that $\rho_o = \rho_o(z)$ only.

and

$$\rho_o \bar{u} \frac{\partial \overline{C_p' w'}}{\partial x} = -\rho_o \overline{w'w'} \frac{\partial \bar{C}_p}{\partial z} + \frac{\partial}{\partial y}\left(\rho_o \Lambda \sqrt{K} \frac{\partial \overline{C_p' w'}}{\partial y}\right)$$
$$+ 3 \frac{\partial}{\partial z}\left(\rho_o \Lambda \sqrt{K} \frac{\partial \overline{C_p' w'}}{\partial z}\right) + \frac{\partial}{\partial y}\left(\rho_o \Lambda \sqrt{K} \frac{\partial \overline{C_p' v'}}{\partial z}\right)$$
$$+ \frac{\partial}{\partial z}\left(\rho_o \Lambda \sqrt{K} \frac{\partial \overline{C_p' v'}}{\partial y}\right) - \frac{\rho_o \sqrt{K}}{\Lambda} \overline{C_p' w'}$$
$$+ \mu_o \left(\frac{\partial^2 \overline{C_p' w'}}{\partial y^2} + \frac{\partial^2 \overline{C_p' w'}}{\partial z^2} - \frac{2\overline{C_p' w'}}{\lambda^2}\right)$$
$$- \left(\mu_o + \mu_2\right)\left[\frac{1}{\rho_o}\frac{\partial^2 \rho_o}{\partial z^2} - \frac{2}{\rho_o^2}\left(\frac{\partial \rho_o}{\partial z}\right)^2\right]\overline{C_p' w'}$$
$$+ \frac{\rho_o g}{T_o} \overline{C_p' T'} \qquad (14)$$

These two equations begin to provide some insight into the physics of turbulent flux of a contaminant. The first term on the right, of Eq. (14), $-\rho_o \overline{w'w'} \partial \bar{C}_p / \partial z$, is a production term for $\overline{C_p' w'}$ which shows this flux is generated out of the interaction of the turbulent motion $\overline{w'^2}$ and the mean gradient of concentration. The only other possible production is the last term of (14), $\rho_o g \overline{C_p' T'} / T_o$, which is a production term if $\overline{C_p' T'}$ is positively correlated, i.e., positive fluctuations of C_p are associated with positive temperature fluctuations, and is a dissipation term if $\overline{C_p' T'}$ is negative. This term, of course, simply reflects the effects of buoyancy. The second and third terms on the right side of (13) and (14) represent the diffusion of the flux along the direction of the flux. The fourth and fifth terms represent the transformation of flux in one direction into flux in the orthogonal direction. The sixth term represents the loss of flux due to the tendency-to-isotropy of the turbulent flow. The seventh term represents the molecular diffusion of the flux and the reduction of the

magnitude of the flux by the effects of molecular motion. The eighth term in (14) reflects the fact that, in the presence of a density gradient, the divergence of the flow is nonzero and leads to a small production of flux in the vertical direction.

These equations have produced one new term, $\overline{c_p'T'}$; hence the following equation for $\overline{c_p'T'}$ is required.

3. The pollutant-temperature correlation.

$$\rho_o \bar{u} \frac{\partial \overline{c_p'T'}}{\partial x} = -\rho_o \overline{w'T'} \frac{\partial \bar{c}_p}{\partial z} - \rho_o \overline{c_p'w'} \frac{\partial \bar{T}}{\partial z} + \frac{\partial}{\partial y}\left(\rho_o A \sqrt{K} \frac{\partial \overline{c_p'T'}}{\partial y}\right)$$

$$+ \frac{\partial}{\partial z}\left(\rho_o A \sqrt{K} \frac{\partial \overline{c_p'T'}}{\partial z}\right) + \mu_o \left(\frac{\partial^2 \overline{c_p'T'}}{\partial y^2} + \frac{\partial^2 \overline{c_p'T'}}{\partial z^2} - \frac{2\overline{c_p'T'}}{\lambda^2}\right) \qquad (15)$$

Again, the first two terms are production terms for $\overline{c_p'T'}$, the second two are eddy diffusion terms, and the fifth represents molecular diffusion and a reduction of $\overline{c_p'T'}$.

These four equations provide the diffusion model for material released continuously from a point source. Since the present test of the model is for an infinite cross-wind line source, we may simply note that all of the terms in Eq. (13) are zero for this source configuration. Equations (12), (14), and (15) then constitute the diffusion model.* In order to solve these three equations, we require prediction equations for $\bar{u}(z)$, $\bar{T}(z)$, $\overline{u'^2}$, $\overline{v'^2}$, $\overline{w'^2}$, $\overline{u'w'}$, $\overline{u'T'}$, $\overline{w'T'}$, and $\overline{T'^2}$. Since these are the same equations required for prediction of the turbulent flow, independent of the presence of a passive pollutant, we may utilize the invariant model of

*We have named this diffusion model LPD, the acronym for Line Pollution Diffusion. The model for a point source has been designated as SPD for Spatial Pollution Diffusion

turbulent boundary layer flow directly. This model has been discussed extensively by Donaldson. Including the reprint attached as Appendix A to this report. (For another discussion of the physical meaning of the terms appearing in this model, the reader is referred to Lumley and Panofsky [6].) For completeness, we repeat the turbulent model equations as used for the present tests.

4. The equations for the mean wind and temperature.

$$\rho_o \frac{\partial \bar{u}}{\partial t} = \mu_o \frac{\partial^2 \bar{u}}{\partial z^2} - \frac{\partial}{\partial z}\left(\rho_o \overline{u'w'}\right) \tag{16}$$

$$\rho_o \frac{\partial \bar{T}}{\partial t} = \mu_o \frac{\partial^2 \bar{T}}{\partial z^2} - \frac{\partial}{\partial z}\left(\rho_o \overline{T'w'}\right) \tag{17}$$

5. The turbulent energy equations.

$$\rho_o \frac{\partial \overline{u'u'}}{\partial t} = -2\rho_o \overline{u'w'} \frac{\partial \bar{u}}{\partial z} + \frac{\partial}{\partial z}\left(\rho_o \Lambda \sqrt{K} \frac{\partial \overline{u'u'}}{\partial z}\right) - \rho_o \frac{\sqrt{K}}{\Lambda}\left(\overline{u'u'} - \frac{K}{3}\right)$$

$$+ \mu_o \frac{\partial^2 \overline{u'u'}}{\partial z^2} - \frac{2\mu_o \overline{u'u'}}{\lambda^2} \tag{18}$$

$$\rho_o \frac{\partial \overline{v'v'}}{\partial t} = \frac{\partial}{\partial z}\left(\rho_o \Lambda \sqrt{K} \frac{\partial \overline{v'v'}}{\partial z}\right) - \rho_o \frac{\sqrt{K}}{\Lambda}\left(\overline{v'v'} - \frac{K}{3}\right)$$

$$+ \mu_o \frac{\partial^2 \overline{v'v'}}{\partial z^2} - \frac{2\mu_o \overline{v'v'}}{\lambda^2} \tag{19}$$

$$\rho_o \frac{\partial \overline{w'w'}}{\partial t} = \frac{\partial}{\partial z}\left(3\rho_o \Lambda\sqrt{K}\,\frac{\partial \overline{w'w'}}{\partial z}\right) - \rho_o \frac{\sqrt{K}}{\Lambda}\left(\overline{w'w'} - \frac{k}{3}\right)$$

$$+ 2\,\frac{\partial \rho_o}{\partial z}\left(\Lambda\sqrt{K}\,\frac{\partial \overline{w'w'}}{\partial z}\right) + 3\,\frac{\partial}{\partial z}\left(\rho_o \Lambda\sqrt{K}\,\frac{\partial \overline{w'w'}}{\partial z}\right)$$

$$+ \mu_o \frac{\partial^2 \overline{w'w'}}{\partial z^2} - \frac{\partial \mu_o}{\partial z}\frac{\overline{w'w'}}{\lambda^2}$$

$$- 2\left(\mu_o + \mu_2\right)\left\{\overline{w'w'}\left[\frac{\partial}{\partial z}\left(\frac{1}{\rho_o}\frac{\partial \rho_o}{\partial z}\right) - \frac{1}{\rho_o^2}\left(\frac{\partial \rho_o}{\partial z}\right)^2\right]\right\}$$

$$+ \frac{2\rho_o g}{T_o}\,\overline{w'T'} \qquad (20)$$

6. The momentum and heat flux equations

$$\rho_o \frac{\partial \overline{u'w'}}{\partial t} = -\rho_o \overline{w'w'}\,\frac{\partial \bar{u}}{\partial z} + 3\,\frac{\partial}{\partial z}\left(\rho_o \Lambda\sqrt{K}\,\frac{\partial \overline{u'w'}}{\partial z}\right)$$

$$- \rho_o \frac{\sqrt{K}\,\overline{u'w'}}{\Lambda} + \Lambda\sqrt{K}\,\frac{\partial \overline{u'w'}}{\partial z}\,\frac{\partial \rho_o}{\partial z}$$

$$+ \mu_o \frac{\partial^2 \overline{u'w'}}{\partial z^2} - \frac{\partial \mu_o}{\partial z}\frac{\overline{u'w'}}{\lambda^2}$$

$$- \left(\mu_o + \mu_2\right)\left\{\overline{u'w'}\,\frac{\partial}{\partial z}\left(\frac{1}{\rho_o}\frac{\partial \rho_o}{\partial z}\right) - \frac{\overline{u'w'}}{\rho_o^2}\left(\frac{\partial \rho_o}{\partial z}\right)^2\right\}$$

$$+ \frac{\rho_o g}{T_o}\,\overline{u'T'} \qquad (21)$$

$$\rho_o \frac{\partial \overline{w'T'}}{\partial t} = -\rho_o \overline{w'w'}\,\frac{\partial \bar{T}}{\partial z} - \rho_o\,\overline{w'T'}\,\frac{\partial \bar{w}}{\partial z} + \frac{\partial}{\partial z}\left(\rho_o \Lambda\sqrt{K}\,\frac{\partial \overline{w'T'}}{\partial z}\right)$$

$$- \frac{\rho_o \sqrt{K}\,\overline{w'T'}}{\Lambda} + \mu_o \frac{\partial^2 \overline{w'T'}}{\partial z^2} - \frac{\partial \mu_o}{\partial z}\frac{\overline{w'T'}}{\lambda^2} \qquad (22)$$

$$\rho_o \frac{\partial \overline{w'T'}}{\partial t} = -\rho_o \overline{w'w'} \frac{\partial \overline{T}}{\partial z} + 3 \frac{\partial}{\partial z}\left(\rho_o \Lambda \sqrt{K} \frac{\partial \overline{w'T'}}{\partial z}\right)$$
$$- \frac{\rho_o \sqrt{K}\, \overline{w'T'}}{\Lambda} + \mu_o \frac{\partial^2 \overline{w'T'}}{\partial z^2} - \frac{2\mu_o \overline{w'T'}}{\lambda^2}$$
$$- \left(\mu_o + \mu_2\right)\left\{\overline{w'T'} \frac{\partial}{\partial z}\left(\frac{1}{\rho_o} \frac{\partial \rho_o}{\partial z}\right) - \frac{\overline{w'T'}}{\rho_o^2}\left(\frac{\partial \rho_o}{\partial z}\right)^2\right\}$$
$$+ \frac{\rho_o g}{T_o} \overline{T'^2} \tag{23}$$

7. The variance of the temperature fluctuations

$$\rho_o \frac{\partial \overline{T'^2}}{\partial t} = -2\rho_o \overline{w'T'} \frac{\partial \overline{T}}{\partial z} + \frac{\partial}{\partial z}\left(\rho_o \Lambda \sqrt{K} \frac{\partial \overline{T'^2}}{\partial z}\right)$$
$$+ \mu_o \frac{\partial^2 \overline{T'^2}}{\partial z^2} - \frac{2\mu_o \overline{T'^2}}{\lambda^2} \tag{24}$$

Following Rotta [7], we complete the model by writing

$$\Lambda = \lambda \sqrt{a + b\mathrm{Re}_\Lambda} \tag{25}$$

where a and b are constants, and

$$\mathrm{Re}_\Lambda = \frac{\rho_o \Lambda \sqrt{K}}{\mu_o} \tag{26}$$

For our present purposes, Λ has been retained as a free parameter.

4. SOME RELATIONSHIPS BETWEEN SECOND-ORDER AND FIRST-ORDER CLOSURE MODELS

One of the purposes of second-order closure is to retain more specific information regarding the structure of turbulent flows, out of which, hopefully, increased physical insights can be gained for the improvement of first-order closure models of turbulent fluid flow. These relationships between first- and second-order closure models are most readily seen by comparing the predictions of the two types of models for specific physical processes. For our present purposes, we choose to compare predictions of the vertical flux of horizontal momentum $\rho_o \overline{u'w'}$ and the vertical flux of heat $\rho_o c \overline{w'T'}$ which are given by

$$\rho_o \overline{u'w'} = - \rho_o K_m^* \left| \frac{\partial \bar{u}}{\partial z} \right| \tag{27}$$

and

$$c\rho_o \overline{w'T'} = - \rho_o c K_H^* \left(\frac{\partial \bar{T}}{\partial z} \right) \tag{28}$$

where $\bar{T}$ is potential temperature and c is the specific heat at constant pressure. Equations (27) and (28) are best interpreted as the definitions of K_m^*, the eddy diffusivity for momentum, and K_H^*, the eddy diffusivity for heat, both of which may be functions of height, stability, wind speed, surface roughness, and each other. We may, therefore, focus attention on comparisons of first- and second-order closure models for K_m^* and K_H^*; the latter are <u>defined</u> as

$$K_m^* = - \frac{\overline{u'w'}}{|\partial \bar{u}/\partial z|} \tag{29}$$

and

$$K_H^* = - \frac{\overline{w'T'}}{(\partial \bar{T}/\partial z)} \tag{30}$$

Since all of the terms on the right-hand side of Eqs. (29) and (30) can be, and have been, measured in the lower atmosphere, we have relatively good empirical evidence of the values of K_m^* and K_H^* in that layer and their general behavior as a function of height, wind speed, stability, and surface roughness. The predictions of first-order and second-order closure models for K_m^* and K_H^* may, therefore, be tested against reality, as well as against each other.

Various empirical and semi-empirical forms for K_m^* and K_H^* have been proposed (cf., Priestley [8], Pasquill [9], Lumley and Panofsky [6], and Pandolfo [10]). From these, we choose to compare the following forms of first-order closure models:

"Profile" Model

$$K_m^* = k^2 z^2 \left| \frac{\partial \bar{u}}{\partial z} \right| \left(1 \mp \alpha R_i\right)^{\pm 2} \tag{31}$$

and

"Similarity Theory" Model

$$K_m^* = k^2 z^2 \left| \frac{\partial \bar{u}}{\partial z} \right| \left(1 + \frac{\beta z}{L}\right)^{-2} \tag{32}$$

where R_i is the Richardson number and L is the Monin-Obukhov length. These parameters are defined by

$$R_i = \frac{g}{\bar{T}} \frac{(\partial \bar{T}/\partial z)}{(\partial \bar{u}/\partial z)^2} \tag{33}$$

and

$$L = - \frac{(-\overline{u'w'})^{3/2} \bar{T}}{kg\ \overline{w'T'}} \tag{34}$$

The choice of sign in Eq. (31) is determined by the sign of the Richardson number; the upper sign is chosen when $R_i \geq 0$, and the lower sign when $-0.05 < R_i < 0$. (Since both Eqs. (31) and (32) are restricted to a relatively small range of

stability about neutral ($R_i = 0$, $L = \infty$), we shall restrict the comparison between first- and second-order closure models to that range, also.)

The predictions of K_m^* and K_H^* from the invariant model may be derived directly from Eqs. (21) and (23), if we assume an equilibrium condition has been reached, i.e., $\partial\overline{u'w'}/\partial t$ and $\partial\overline{w'T'}/\partial t$ are equal to zero. Neglecting all of the molecular terms except the molecular dissipation (which is tantamount to restricting the comparison to heights well above the laminar sublayer), we solve for $\overline{u'w'}$ and $\overline{w'T'}$ from Eqs. (21) and (23) and form K_m^* and K_H^*. The results are:

"Invariant" Model

$$K_m^* = \frac{\overline{w'^2}\,\frac{\partial \bar{u}}{\partial z} - \frac{3}{\rho_o}\frac{\partial}{\partial z}\left(\rho_o \Lambda\sqrt{K}\,\frac{\partial \overline{u'w'}}{\partial z}\right) - \frac{g}{T_o}\,\overline{u'T'}}{\left(\frac{2\mu_o}{\rho_o \lambda^2} + \frac{\sqrt{K}}{\Lambda}\right)\frac{\partial \bar{u}}{\partial z}} \tag{35}$$

and

$$K_H^* = \frac{\overline{w'^2}\,\frac{\partial \bar{T}}{\partial z} - \frac{3}{\rho_o}\frac{\partial}{\partial z}\left(\rho_o \Lambda\sqrt{K}\,\frac{\partial \overline{w'T'}}{\partial z}\right) + \frac{g}{\rho_o T_o}\,\overline{T'^2}}{\left(\frac{2\mu_o}{\rho_o \lambda^2} + \frac{\sqrt{K}}{\rho_o \Lambda}\right)\frac{\partial \bar{T}}{\partial z}} \tag{36}$$

Focusing attention on Eq. (35) which we wish to compare with Eqs. (31) and (32), we may note immediately that the eddy diffusivity derived from second-order closure will depend upon the following processes and coefficients:

1. The local production of shear stress by the term $\overline{w'^2}\partial\bar{u}/\partial z$

2. The local diffusion of shear stress, by the term

$$\frac{3}{\rho_o}\frac{\partial}{\partial z}\left(\rho_o \Lambda\sqrt{K}\,\frac{\partial \overline{u'w'}}{\partial z}\right)$$

3. The local production (or dissipation) of shear stress, by the longitudinal turbulent heat flux as measured by $g\overline{u'T'}/T_o$ (this is a production term if $\overline{u'T'}$ is negative and is dissipative if $\overline{u'T'}$ is positive).

4. The coefficient of the essentially local dissipation of shear stress by molecular effects, $2\mu_o/\rho_o\lambda^2$. *

5. The coefficient of the tendency to isotropy of the shear stress $\sqrt{K}/\Lambda$. This coefficient depends upon the square root of twice the local turbulent kinetic energy which is measured by K , and by the spatial scale of the motion Λ which is not determined locally.

6. The local mean wind speed shear $\partial\bar{u}/\partial z$.

Similar functional terms appear in Eq. (36). One important distinction arises in the prediction of K_H^* , however, in that the buoyancy term $(g/T_o)T'^2$ is always positive definite (or zero). The presence of temperature fluctuations always enhances the value of K_H^* while they may increase or decrease K_m^* depending upon whether $\overline{u'T'}$ is negative or positive. We should also note that K_m^* is not defined for $\partial\bar{u}/\partial z = 0$ and K_H^* is not defined for $\partial\bar{T}/\partial z = 0$. The latter condition is not significant, since all of the terms in Eq. (36) are zero for $\partial\bar{T}/\partial z = 0$; i.e., there is no turbulent vertical heat flux in a neutrally stratified atmosphere. This is not the case for K_m^* when $\partial\bar{u}/\partial z = 0$, however, since only the local production of shear stress necessarily goes to zero under this condition. Shear stress produced elsewhere may be diffused into this region,

---

*λ is of the order of 0.1 meters in the lower atmosphere but may be as large as 10 meters in the stratosphere.

and shear stress may be dissipated or produced in the presence of fluctuations of the potential temperature and the longitudinal component of velocity.

These portrayals of the complicated physical processes which determine the effective eddy diffusivity point immediately to the tremendous requirements which first-order closure imposes upon either the Richardson number or the Monin-Obukhov scale length. When viewed from the perspective of second-order closure, the surprising feature is that first-order closure models have been as successful as they have been! Since the first-order closure models do not separate the physical processes of production, diffusion, dissipation, and the tendency-to-isotropy of shear stress or heat flux, term-by-term comparison is not possible, and we must depend upon calculations and observations of K_m^* and K_H^* to proceed with any general comparison. However, at the present stage of development, we may investigate the very special case of a constant shear stress layer in a neutrally stratified atmosphere, a situation for which K_H^* is not defined. This is the case for which the first-order closure models are most reliable, and equivalence between first- and second-order closure models can be expected.

4.1 K_m^* from First- and Second-Order Closure Models in a Neutrally Stratified, Constant Shear Stress Layer

Under the conditions $\partial\overline{T}/\partial z = 0$ and $\partial\overline{u'w'}/\partial z = 0$, the form of K_m^* from the invariant model is

$$K_m^* = \frac{\overline{w'^2}}{\left(\frac{2\mu_o}{\rho_o\lambda^2} + \frac{\sqrt{\overline{K}}}{\Lambda}\right)} \tag{37}$$

and both the "profile" model [Eq. (31)] and the "similarity theory" model [Eq. (32)] reduce to the form

$$K_m^* = k^2 z^2 \left(\frac{\partial \bar{u}}{\partial z}\right) \tag{38}$$

Equation (37) may be simplified further by noting that for heights well above the laminar sublayer $2\mu_o/\rho_o\lambda^2 \ll \sqrt{K}/\Lambda$. Then the invariant model predicts K_m^* as

$$K_m^* = \frac{\overline{w'^2}\Lambda}{\sqrt{K}} \tag{39}$$

and we have equivalence among the "profile" model, the "similarity theory" model, and the "invariant" model, if

$$k^2 z^2 \left|\frac{\partial \bar{u}}{\partial z}\right| = \frac{\overline{w'^2}\Lambda}{\sqrt{K}} \tag{40}$$

A physical interpretation of Eq. (40) is seriously hampered by the obscuration of the physical construct of the left-hand side and by the lack of specificity for Λ in terms of fluid flow parameters, on the right-hand side. A simple dimensional comparison suggests that $\overline{w'^2} \sim z^2(\partial\bar{u}/\partial z)^2$ and $\Lambda/\sqrt{K} \sim (\partial\bar{u}/\partial z)^{-1}$, but how $k^2 z^2 \partial\bar{u}/\partial z$ is apportioned between these two terms is not immediately evident.

From another point of view, the requirement that the shear stress be constant with height leads to

$$\frac{\overline{w'^2}\Lambda}{\sqrt{K}}\left(\frac{\partial \bar{u}}{\partial z}\right) = \text{constant} \tag{41}$$

If $\overline{w'^2}/\sqrt{K}$ is constant, i.e., the vertical component of the turbulent kinetic energy is a fixed fraction of the total turbulent kinetic energy, we recover the logarithmic wind profile (appropriate to this case) only if $\Lambda \sim z$.

Since all of the terms in Eq. (40), other than Λ, are known or measurable, we can determine the value of Λ/z from observations of $\partial\bar{u}/\partial z$, $\overline{w'^2}$, and K in neutrally stratified, constant shear stress layers of the atmosphere.

Limited observations to date suggest $\Lambda \simeq 0.7z$, but more general observations over a variety of terrain are required before this relationship can be confidently assessed from experimental data.

At the present stage of development, it would, therefore, appear most profitable to view Eq. (40) as the definition for a reference value of Λ, say Λ_o, where Λ_o is interpreted as the value of this scale length which assures equivalence between first- and second-order closure models for the special case of a neutrally stratified atmospheric layer for which the shear stress is constant.

We must note at this point, however, that in this early version of the invariant model we have assumed there is a single scale length Λ which is appropriate to both the diffusion of shear stress and to the tendency to isotropy of the shear stress. This assumption is not necessarily valid and we should point out that the value of Λ appropriate to Eq. (41) is the value of the scale length which enters into the determination of tendency to isotropy. Modeling of laboratory scale flows seems to suggest that this scale length is about ten times the scale length appropriate to the diffusion of shear stress. Further study of these two scale lengths for atmospheric flow is required.

Beyond this limiting comparison between first- and second-order closure models, present attention is being directed to calculations, with the invariant model, which match observed values of $\overline{u'w'}$ and $\overline{w'T'}$ as a function of height in diabatic boundary layers. From such calculations all of the inputs necessary to establish the vertical profiles of the Monin-Obukhov length L and of α and β and their dependence upon stability, wind velocity and shear, etc., can be established. Once the credibility of the second-order closure model has been established, it will be an extremely valuable tool in assessing the adequacy of first-order closure

models. If these should prove adequate, particularly in arbitrarily stratified atmospheres, the invariant model will once again be useful in specifying the coefficients of first-order closure models for these situations.

5. INITIAL TESTS OF THE MODEL

Since the basic information normally available for the atmospheric surface layer is the mean profiles of wind and temperature, the method of solution adopted for the calculations of turbulence structure was to decouple Eqs. (16) and (17) and solve Eqs. (18) through (25) subject to the observed (constant) values of $\bar{u}(z)$ and $\bar{T}(z)$. A small initial turbulence (u'^2, v'^2, w'^2) was introduced, and this portion of the model was run until all the turbulent energies and turbulent fluxes came into equilibrium; i.e., the local time derivatives went to zero.

In an earlier phase of this work,* data were obtained from the Air Force Cambridge Research Laboratories (AFCRL) which included mean wind and temperature profiles, as well as careful measurements of the turbulent energies and fluxes in the first 100 feet above a flat surface in Kansas. Although no diffusion data are available in connection with the AFCRL measurements, one of these runs was selected for diffusion calculations. This run has been designated "Coté 40." It was characterized by an unstable lapse rate from the surface to about 30 feet and was neutral above that height. The input information $\bar{u}$, $\bar{T}$, and Λ and the calculated values of $\overline{w'T'}$ and $\overline{w'w'}$ for this test case are shown in Figure 1.

In order to test the model under other stability conditions, a second case was chosen for which the lower atmosphere was stably stratified and for which detailed measurements of the vertical distribution of a tracer material were available out to 5000 feet from an elevated point source. These measurements were made by Hilst and Simpson at Hanford and were reported in the Journal of Meteorology [11]. Only the mean wind and temperature profiles were available for this case.

---

*A.R.A.P. Report No. 162, NASA CR-111962, NASA Contract No. NAS1-10192

The input information and the calculated turbulence and flux structure are shown in Figure 2.

With these choices, the initial tests of the model bracket the stable to neutral or slightly unstable range. Extension into the unstable case does not appear warranted until a better match between observed and calculated turbulence structures is achieved by the refinements presently underway.

Having modeled the structure of turbulence, the diffusion portion of the model was run and the predicted concentration profiles and the moments of these profiles were compared with experimental data. For this portion of the test, the line source was placed at 200 feet above ground level and the initial vertical concentration profile was specified as a full gaussian with unit variance and a central value of 1.0. Printouts of the predicted concentration profiles, the moments of these profiles, and the vertical fluxes of material were required at distances of 500, 1000, 2500, 5000, and 10,000 feet from the source.

With this wealth of detail, the calculated results far outstrip the available information from observational data. However, a comparison with several experimental measurements can be made by way of the variance of the concentration distribution σ_z^2 (or σ_z) which is frequently reported. We can, therefore, readily check the model's order-of-magnitude estimates of vertical diffusion. Beyond this, we must depend upon a few observations and intuition in checking the predicted concentration profiles directly.

5.1 An Example

In order to get an initial estimate of the behavior of the diffusion model and to demonstrate the output information, the first calculation was run under the assumption that a

single scale length Λ was appropriate to the diffusion simulation as well as for the generation of the field of turbulence. Using the unstable to neutral case (Cote 40, Λ_{max} = 60 feet), the vertical profiles of concentration were calculated to a distance of 10,000 feet downwind from the source line. The basic results of this trial calculation are shown in Figure 3 in the form of the concentration profiles at x = 500, 5000, and 10,000 feet; the values of the axial concentration, $\overline{C}_{p_{max}}$; and the first four moments of the concentration distributions.

Inspection of the concentration profiles shows the expected vertical transfer upward and downward, reflection at the ground surface, and the establishment of an essentially uniformly mixed layer below the height of the source. An immediately disturbing feature, however, is the presence of a narrow band of high concentration at the source height, a feature which maintains abnormally high values of the axial concentration. It would appear that with this initial choice of Λ_{max} and the constants a and b which relate Λ_{max} to the dissipation scale length λ, the model exhibits a pathological tendency to minimize the turbulent flux near the axis of the cloud, even though relatively large fluxes are calculated outside this region. This problem, which is discussed further in Section 5.3, has been of primary concern and has led to a generalization of the scale lengths along two lines: 1) the adoption of separate scale lengths for turbulence generation and for diffusion, and 2) a reëxamination of the relative magnitudes of the scale lengths associated with the dissipation of turbulent energy and fluxes as compared with the pressure diffusion and tendency-towards-isotropy terms. The first approach, which is largely empirical and is aimed at an estimation of the sensitivity of $\overline{C}_p$ to scale lengths, is reported here. The second approach is the subject of a report by Donaldson [12].

Beyond this immediate difficulty, the trial calculations of the second moment of the concentration distribution σ_z^2 exhibit all of the characteristics of classical diffusion theory. As can be seen from the plot of σ_z^2 vs. x in Figure 4, after an initial period during which the fluxes of material $\overline{c'w'}$ are brought into equilibrium, σ_z^2 increases as the square of the distance and, as σ_z^2 approaches Λ_{max}^2, this dependence goes over to the classical Fickian diffusion rate, with $\sigma_z^2 \sim x$. The asymptotic behavior of σ_z^2 is, therefore, analogous to the behavior predicted by the statistical theory of turbulence and we may associate Λ_{max} with the scale length of the turbulence.

If we wish to do so, every term explicit in the model may be printed out and detailed checks made of their relative magnitudes and their spatial and time derivatives. To illustrate this capacity for detailed analyses of complex situations, we have plotted the vertical profiles of the turbulent flux of material at x = 5000, 7000, and 10,000 feet in Figure 5. The manner and rate at which the initially downward flux below the plume goes over to an upward flux and establishes a completely mixed layer is clearly portrayed by these calculations.

With these general features and behavior of the diffusion model in hand, attention was turned to experimentation with the only free parameter available, Λ, and to a first assessment of the effects of stability and wind shear on the vertical diffusion predicted by the model.

5.2 An Initial Test of the Effect of Stability

As a first attempt to determine the model's prediction of the effect of stability on vertical diffusion, the model was rerun using the same assumptions as before, but inputting the stable turbulence field as derived from the Hanford data. Again, the scale length Λ_{max} was set equal to 60 ft, the value chosen for the turbulence generation run. The profiles

of concentration at x = 500, 5000, and 10,000 feet are shown in Figure 6 and may be compared directly with Figure 3.

The values of σ_z^2 are shown in Figure 7 and, for convenience, comparable values of σ_z^2 for the neutral case (Fig.4) are replotted here also. Finally, experimental values of σ_z^2 for neutral and stable atmospheres are plotted in Figure 7, as an initial verification of the model predictions. As can be seen from these comparisons, surprisingly realistic values of σ_z^2 are obtained for the neutral case. In the stable case, the model prediction is clearly overpredicting σ_z^2 when compared with the Hanford observations, but σ_z^2 vs. x has the right shape.

It is interesting to note that the model predicts an equivalent growth rate for the neutral and stable diffusion cases until σ_z^2 reaches approximately 1000 ft^2. Then the growth rates diverge rapidly, with the further vertical diffusion of the cloud much slower in the stably stratified atmosphere. This result suggests that vertical diffusion is relatively independent of stability and wind shear while the cloud is small, a result which is observed in the Hanford experiments and which conforms to the expectation that the large-scale turbulent eddies are selectively suppressed by stable temperature stratification (cf., Lumley and Panofsky [6]).

Considering the sweeping nature of the assumption that a single scale length and the mean profiles of wind and temperature correctly model all facets of the structure of boundary layer turbulence and the diffusion of material embedded in that turbulence, this initial test can only be considered remarkable and promising. We can, therefore, undertake further tests and development of the model with confidence.

5.3 The Sensitivity of Diffusion to the Scale Length

Having demonstrated a generally credible simulation of turbulent diffusion, attention was turned to the anomalous behavior of the diffusion prediction near the core of the diffusing cloud. For the simplified, two-dimensional model which we are testing, the equation for the prediction of the rate of change of local turbulent fluxes of material (Eq. (14)) may be written

$$\rho_0 \bar{u} \frac{\partial \overline{C_p'w'}}{\partial x} = -\rho_0 \overline{w'w'} \frac{\partial \bar{C}_p}{\partial z} + \frac{\partial}{\partial z}\left(\rho_0 \sqrt{E}\, \frac{\partial \overline{C_p'w'}}{\partial z}\right) - \frac{\rho_0 \sqrt{E}}{\Lambda} \overline{C_p'w'} + \mu_0\left(\frac{\partial^2 \overline{C_p'w'}}{\partial z^2} - \frac{\overline{C_p'w'}}{\lambda^2}\right) - \left(\mu_0 + \mu_2\right)\left\{\frac{1}{\rho_0}\frac{\partial^2 \rho_0}{\partial z^2} - \frac{2}{\rho_0^2}\left(\frac{\partial \rho_0}{\partial z}\right)^2\right\}\overline{C_p'w'} + \frac{\rho_0^2}{\rho_0}\overline{C_p'T'} \qquad (14)$$

At the elevation of the core of the cloud (200 feet above ground), all of the molecular terms are negligible and, for the cases tested, $\overline{C_p'T'}$ is one to two orders of magnitude less than $\overline{C_p'w'}$. In testing the behavior of the model, we may, therefore, focus attention on the first three terms of the above equation for $\rho_0 \bar{u}\,\partial\overline{C_p'w'}/\partial x$.

The first term, $-\rho_0\overline{w'w'}(\partial \bar{C}_p/\partial z)$, is a production term and represents the creation of flux, or correlation between C_p' and w', out of the mean gradient of $\bar{C}_p$ and the vertical component of turbulence. We note particularly that this production rate depends upon the scale length Λ only through the production of vertical velocity fluctuations $\overline{w'w'}$, a turbulence field which should be independent (under our present assumptions of a chemically and radiatively inert diffusing material) of the distribution of $\bar{C}_p$. The local production of turbulent flux depends, therefore, only on the

scale length associated with the production of turbulent motions and the local mean gradient of the diffusing material.

The second term, $\partial/\partial z)[\rho_o \Lambda \sqrt{K}(\partial \overline{C_p'w'}/\partial z)]$, represents a diffusive process, in particular, the diffusion of the flux $\overline{C_p'w'}$ along the gradient of that flux. Since ρ_o, Λ, and $\sqrt{K}$ are only very slowly varying functions of z while $\overline{C_p'w'}$ varies rapidly with z near the core of the cloud (see Fig. 5), the magnitude of this diffusion of $\overline{C_p'w'}$ depends strongly upon the choice of Λ (all the other terms are explicitly calculated by the model). Now, however, Λ represents that choice of scale length which appropriately models the transport of the flux by turbulent motions and is, therefore, conceivably dependent upon both the scale length of the turbulence and the scale length of the fluctuations of concentration, C_p'. This Λ may, therefore, be different from the scale length of the turbulence, a possibility clearly foreseen in the original development of the model.

Finally, the third significant term, $-(\rho_o \sqrt{K}/\Lambda)\overline{C_p'w'}$, represents the rate of change of turbulent flux due to the tendency towards isotropy in the basic field of turbulent motions. Again, the appropriate scale length for this process may be a hybrid between the turbulence field and the concentration fluctuation field.

These considerations pose the possibility that multiple scale lengths may be required for the model if the many facets of turbulence structure and diffusion which it simulates are to be properly portrayed. A first, and still largely empirical, test of this possibility is to retain a scale length Λ_{turb} which properly portrays the structure of the turbulence, but admit a second scale length Λ_{diff} for the simulation of the diffusion of matter in this field of turbulence.* Since the

*A more fundamental approach is a systematic reëxamination of all the scale lengths by matching the model's predictions to rigorously measured characteristics of the turbulence and diffusion. This approach is being pursued, under a separate contract, for the case of a free jet for which measurements are available. Atmospheric turbulence and diffusion measurements of similar detail are not available.

turbulent motions are independent of the material distributions, this approach poses only complications of interpretation, not inconsistencies.

Without prejudging the exact hybrid nature of Λ_{diff}, we may systematically solve the diffusion equations for various choices of this parameter. Intuitively, we presume the scale length of the turbulence will represent an upper limit on the hybrid Λ_{diff}, but no rigorous arguments have been developed. Since the primary anomaly which initiated this line of inquiry was the slow diffusion of the core of the cloud, we may examine this feature of the model's dependence upon Λ_{diff} first.

Figures 8 and 9 show the predicted values of $\overline{C}_{p_{max}}$ at various distances and for various choices of Λ_{diff}, using the neutral and stable cases, respectively. These results show a strong dependence of $\overline{C}_{p_{max}}$ on Λ_{diff} and, in particular, they reveal an axis of minimum values of $\overline{C}_{p_{max}}$ which depends only on Λ_{diff} and is independent of stability. Mathematically, this result simply states that for each distance of travel, there is a choice of Λ_{diff} which maximizes the model's estimate of the turbulent flux of material out of the core of the plume, and that this choice of Λ_{diff} increases with increasing distance of travel.

This result immediately suggests that the hybrid diffusive scale length Λ_{diff} should be a function of the scale of the cloud, the one characteristic of the diffusion process which also increases with distance. Among the candidate scale lengths of the cloud which might be considered, only one is independent of the functional form of the distribution of the cloud concentration, and this is the standard deviation of that distribution. As another test of the model, we, therefore, chose to key Λ_{diff} on σ_z, and the model was rerun for both the neutral and stable cases under the condition $\Lambda_{diff} = \sigma_z \leq \Lambda_{max} = 60$ ft. The resulting predictions for

σ_z^2 and $\bar{C}_{p_{max}}$ are shown in Figures 10 and 11. As can be seen immediately, this choice for Λ_{diff} had only a minor effect in the neutral case. The decrease of axial concentration is slightly faster than when $\Lambda_{diff} = \Lambda_{max} = 60$ feet in the early stages of cloud travel, but under this more energetic turbulence, diffusion is still rapid and Λ_{diff} goes to its limiting value of 60 feet in the first 1000 feet of travel.

A markedly different result is obtained for the stable case, as is shown in Figure 11. Under this less energetic condition, cloud growth is markedly suppressed and the axial concentration is reduced much more quickly during the first 10,000 ft of travel. However, the prediction of σ_z^2 is still too large beyond 2300 feet, suggesting that $\Lambda_{max} = 60$ ft is an overestimate of this scale length for stably stratified atmospheres.

These results must be considered largely empirical at the present time and subject to amendment as the results of further parameter searches become available (cf., Ref. 12). We may note at this stage, however, that beyond distances of the order of 10,000 feet, the predictions of the invariant model, of the classical eddy diffusivity models, and of the statistical models are indistinguishable for the relatively simple flow and stability patterns adopted for these tests. All predict the classical Fickian diffusion of the cloud. At the shorter distances, however, the invariant model tends to the statistical theory with only a minimum assumption with regard to the dependence of the vertical diffusion coefficient on scale length. No major assumptions or appeal to empiricism are necessary in specifying the effective eddy diffusivity as a function of height and fluid flow conditions. This distinct advantage is, of course, directly attributable to the retention of a large measure of the physics and dynamics of turbulent flow processes in the invariant model. The value of this more rigorous treatment when applied to arbitrary flow and stability conditions - conditions for which empirical relationships become questionable or simply nonexistent - is obvious.

6. A CALCULATION OF THE TIME REQUIRED FOR TURBULENCE TO BECOME FULLY DEVELOPED

A problem of considerable interest in practical air pollution problems is the rate at which the turbulence structure, and, therefore, the diffusion rates, adjust to a major change in the atmospheric flow field. Such changes might be induced by an abrupt change in surface conditions, such as flow from land to water, or rapidly changing pressure gradients with accelerating wind speeds. That portion of the invariant model used to calculate the turbulence field provides the necessary information for estimating the rate at which the atmosphere would respond to such large perturbations.

As an initial experiment to this end, we may postulate the extreme example of an atmosphere which is initially at rest and has any prescribed lapse rate of temperature over the height of interest. At time $t = 0$, this atmosphere is set in laminar motion, and a perturbing turbulent component of motion is superimposed. The model is then run in real time steps until the components of turbulence and turbulent fluxes come into equilibrium.

Two examples of the time history of the development of turbulence, as measured by the maximum values of u'^2, v'^2, $u'^2 + v'^2 + w'^2 = K$, and $\overline{u'w'}$, are shown in Figure 15. The lower part of Figure 15 is for the case of the unstable to neutral atmosphere used in the diffusion calculations; the upper plot is for the case of the Hanford stable atmosphere used earlier.

As can be seen from these plots, the turbulence structure in the neutral atmosphere achieved equilibrium in approximately 50-100 seconds. The stable atmosphere required more than ten times that length of time. This result reflects the strong damping effect of stability on vertical exchange processes and the order-of-magnitude larger turbulent energy generated by the neutral atmosphere. (Note the difference in scales of u'^2, etc.)

Although the conditions of this experiment hardly have a counterpart in nature, this result does suggest a very real difference in the adjustment of the atmosphere as it moves from hot to cold surfaces as compared with movement from cold to hot. The stabilizing effect of motion of warm air over a cold surface can be expected to greatly retard the rate of adjustment of the turbulence.

A more realistic experiment (and one for which necessary programming was started at the end of this phase of work) is to simulate the effects of surface heat flux and calculate the rate of adjustment of turbulence structure which is initially fully developed for the upwind surface temperature conditions. It is planned to complete this study along these more realistic lines in the second phase of work.

7. CONCLUSIONS

As a first assembly of the principles and methods of invariant modeling for the simulation of turbulent diffusion in the atmospheric boundary layer, the results reported here must be considered successful beyond reasonable expectation. What has been demonstrated is that, with only prior knowledge of the mean wind and temperature profiles and using a relationship between the macroscale and the dissipation scale derived for laboratory scale flow, the structure of turbulence and the diffusion of matter are simulated well within an order of magnitude of observed values. In most cases, the verification is within a factor of two, a result which has been achieved for other modeling techniques only after much more effort and resort to empiricism. Perhaps most importantly at this stage of development of the invariant model, all of the classical requirements for asymptotic behavior of the diffusion are met.

In the process of developing these initial tests of the applicability of invariant modeling to atmospheric diffusion, we have begun to identify the avenues of improvement of these simulations. By far the most important of these is the development of a more rigorous basis for estimating the atmospheric scale lengths and the understanding of these scale lengths as they affect the balance of production, diffusion, and dissipation of turbulent fluxes. An extensive reëxamination of the scale lengths associated with laboratory jets has already been initiated (under Air Force and NASA sponsorship). The results of this work will provide a logical starting place for further refinement of scale length choices for atmospheric boundary layer simulation. The objective of this work will be to develop equations for the scale length which depend only on the flow and stability conditions. Since good results have been obtained under relatively crude assumptions regarding

these scale lengths (a result which indicates the primary physics of turbulence and diffusion is accounted for by the local gradients of atmospheric motions, temperature, and pollutant materials), we do not expect a large degree of sensitivity of the scale lengths to these properties. Their further consideration does offer the possibility of improved simulation and, most importantly, confident adaptation of the models to arbitrary flow, stability, and pollutant source configurations.

In the second phase of this development, we propose the following activities.

1. Completion of the simulation model programming for three-dimensional diffusion (appropriate to a continuous point source);

2. The extension of the turbulence generation model to include the depth of the planetary boundary layer and the effects of coriolis forces;

3. The exercising of the model, with improved scale length estimation techniques for arbitrarily stratified planetary boundary layer conditions;

4. The description of the invariant models specifically adapted to atmospheric conditions.

8. REFERENCES

1. Hinze, J.O., 1959: *Turbulence*, McGraw-Hill, New York, 586 pp.

2. Donaldson, Coleman duP., 1971: "Calculation of Turbulent Shear Flows for Atmospheric and Vortex Motions," AIAA Journal *10*, 1, pp. 4-12.

3. Donaldson, Coleman duP., 1969: "A Computer Study of an Analytical Model of Boundary Layer Transition," AIAA Journal *7*, 2, pp. 271-278.

4. Donaldson, Coleman duP. and Sullivan, Roger D., 1970: "Decay of an Isolated Vortex," A.R.A.P. Tech. Memo. 70-6.

5. Donaldson, Coleman duP., Sullivan, Roger D., and Rosenbaum, Harold, 1970: "Theoretical Study of the Generation of Atmospheric Clear Air Turbulence," AIAA Journal *10*, 2, pp. 162-170.

6. Lumley, John L. and Panofsky, Hans A., 1964: *The Structure of Atmospheric Turbulence*, John Wiley & Sons, New York, 239 pp.

7. Rotta, J., 1951: "Statische Theorie Nichthomogener Turbulenz," Zeitschrift für Physik, Vol. 129, p. 547.

8. Priestley, C.H.B., 1959: *Turbulent Transfer in the Lower Atmosphere*, University of Chicago Press, Chicago, 130 pp.

9. Pasquill, F., 1962: *Atmospheric Diffusion*, D. Van Nostrand Co., Ltd., London, 297 pp.

10. Pandolfo, Joseph P., Atwater, Marshall A., and Anderson, Gerald E., 1971: "Prediction by Numerical Models of Transport and Diffusion in an Urban Boundary Layer," Center for the Environment and Man, Hartford.

11. Hilst, Glenn R. and Simpson, C.L., 1958: "Observations of Vertical Diffusion Rates in Stable Atmospheres," J. Meteor. *15*, 1, pp. 125-126.

12. Donaldson, Coleman duP., 1971: "A Progress Report on an Attempt to Construct an Invariant Model of Turbulent Shear Flows," *AGARD Conference Proceedings No. 93 on Turbulent Shear Flows, London, September 1971.*

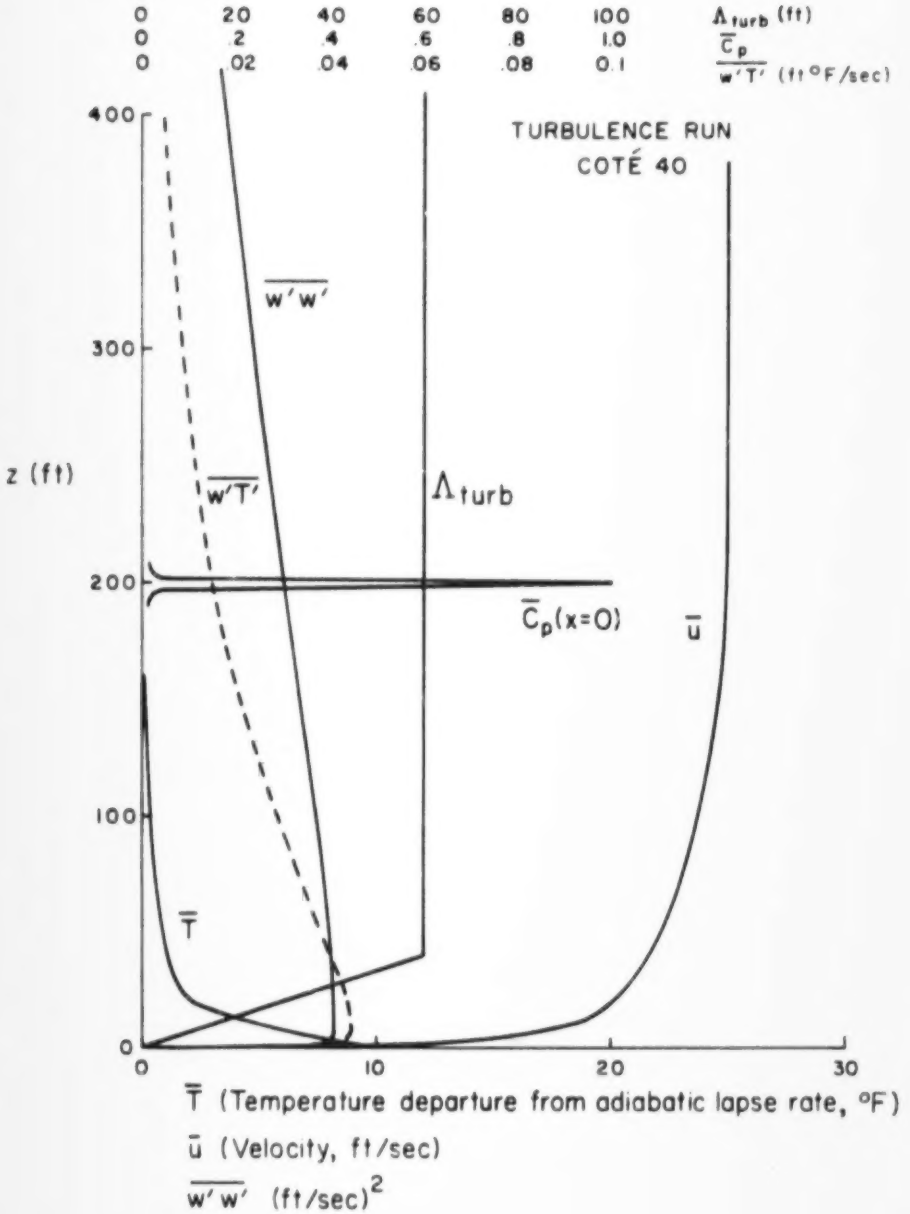

Figure 1. Input values of mean wind speed $\bar{u}$, mean temperature $\bar{T}$, and Λ used to simulate turbulence structure of the lower atmosphere in an unstable-neutral case ($\bar{u}$ and $\bar{T}$ taken from AFCRL data). Predicted profiles of $\overline{w'^2}$ and $\overline{w'T'}$ and the initial concentration profile $\bar{C}_p(z)$ used in later diffusion calculations are also shown.

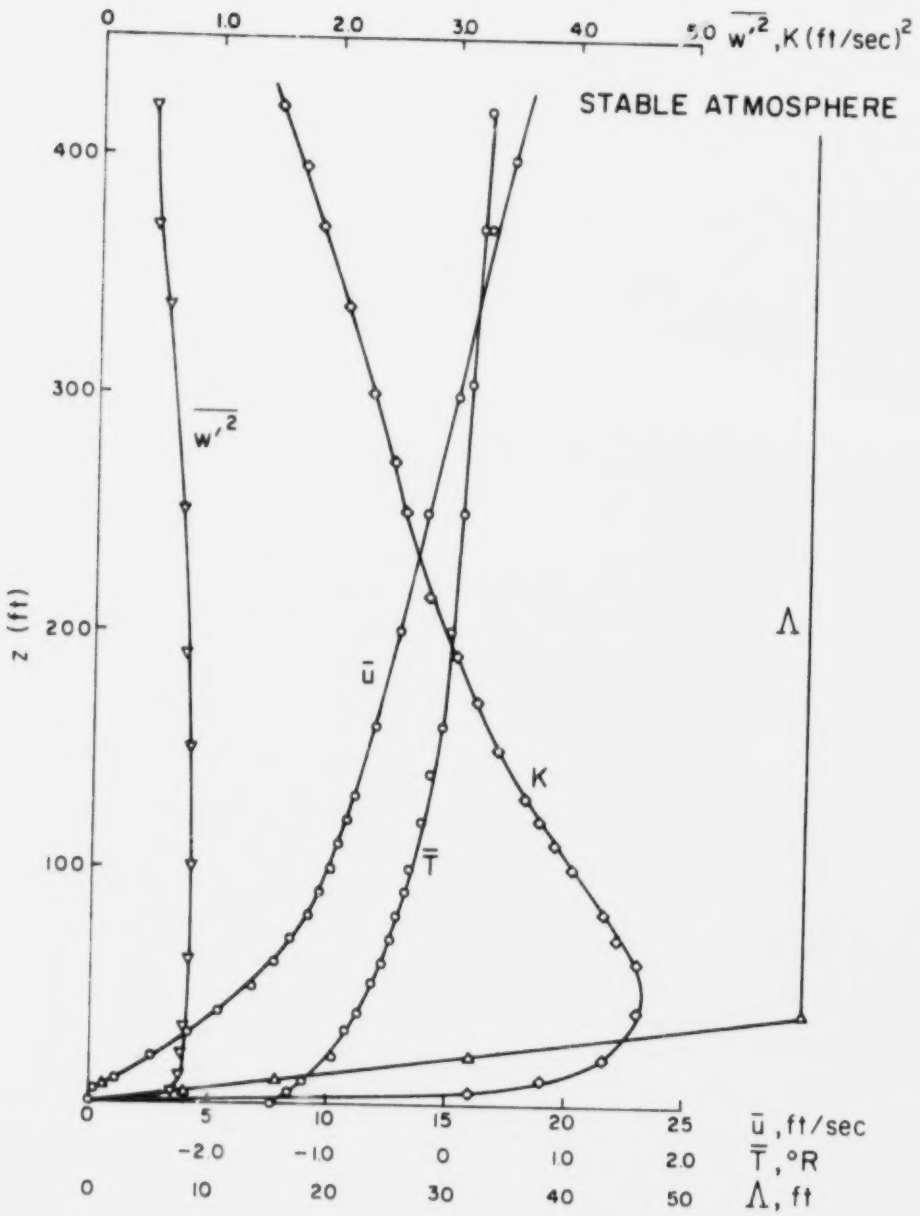

Figure 2. Same as Figure 1 except for a stably stratified atmosphere as measured at Hanford. K is the total turbulent kinetic energy, $\frac{1}{2}(\overline{u'^2} + \overline{v'^2} + \overline{w'^2})$, and is shown to illustrate the relatively large value of $\overline{u'^2} + \overline{v'^2}$, even though $\overline{w'^2}$ is small.

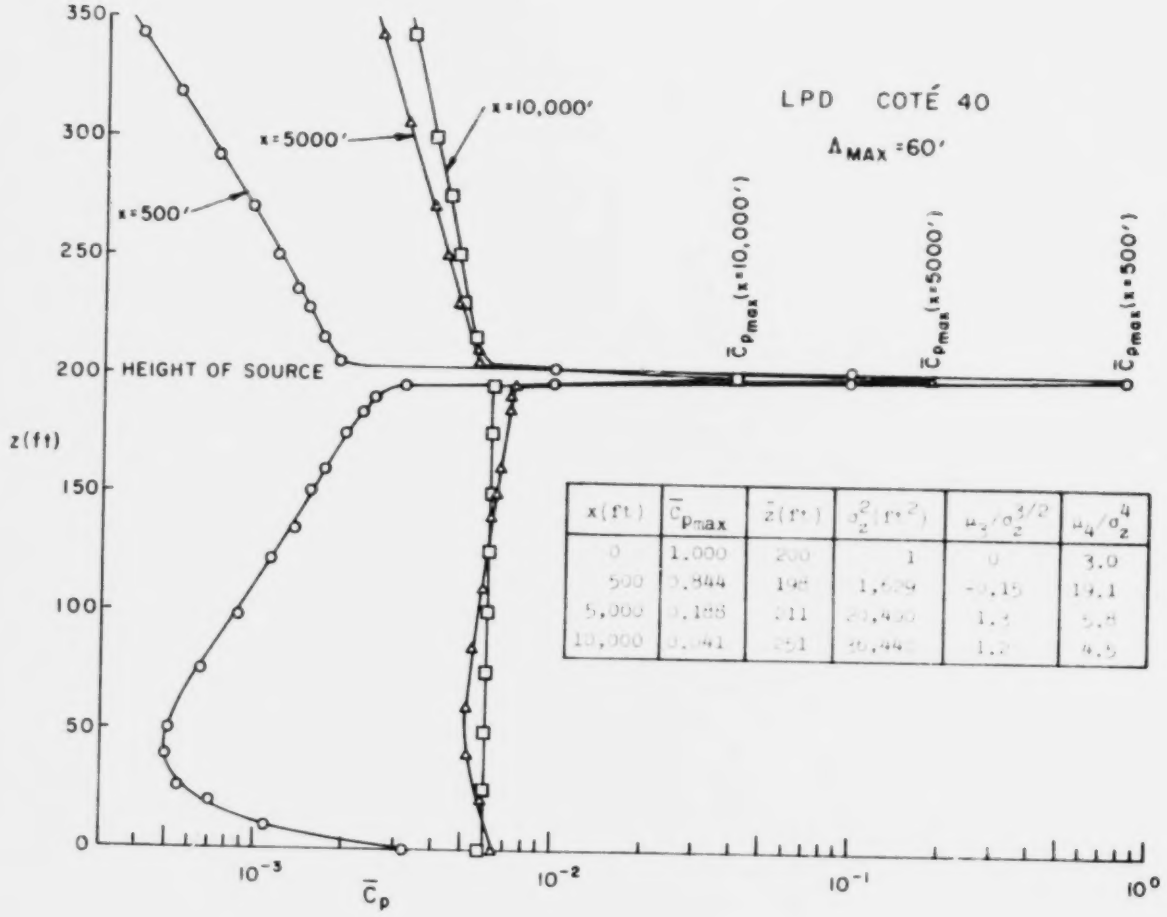

x(ft)	$\bar{C}_{pmax}$	$\bar{z}$(ft)	σ_z^2(ft^2)	$\mu_3/\sigma_z^{3/2}$	μ_4/σ_z^4
0	1.000	200	1	0	3.0
500	0.844	196	1,689	-0.15	14.1
5,000	0.188	211	23,400	1.1	5.8
10,000	0.041	251	35,448	1.2	4.5

Figure 4. Predicted vertical profiles of concentration $\bar{C}_p$ at 500, 5000, and 10,000 feet downwind from a crosswind line source located at a height of 200 feet in a neutral atmosphere. Inset table shows central value and first four moments of $\bar{C}_p(z)$.

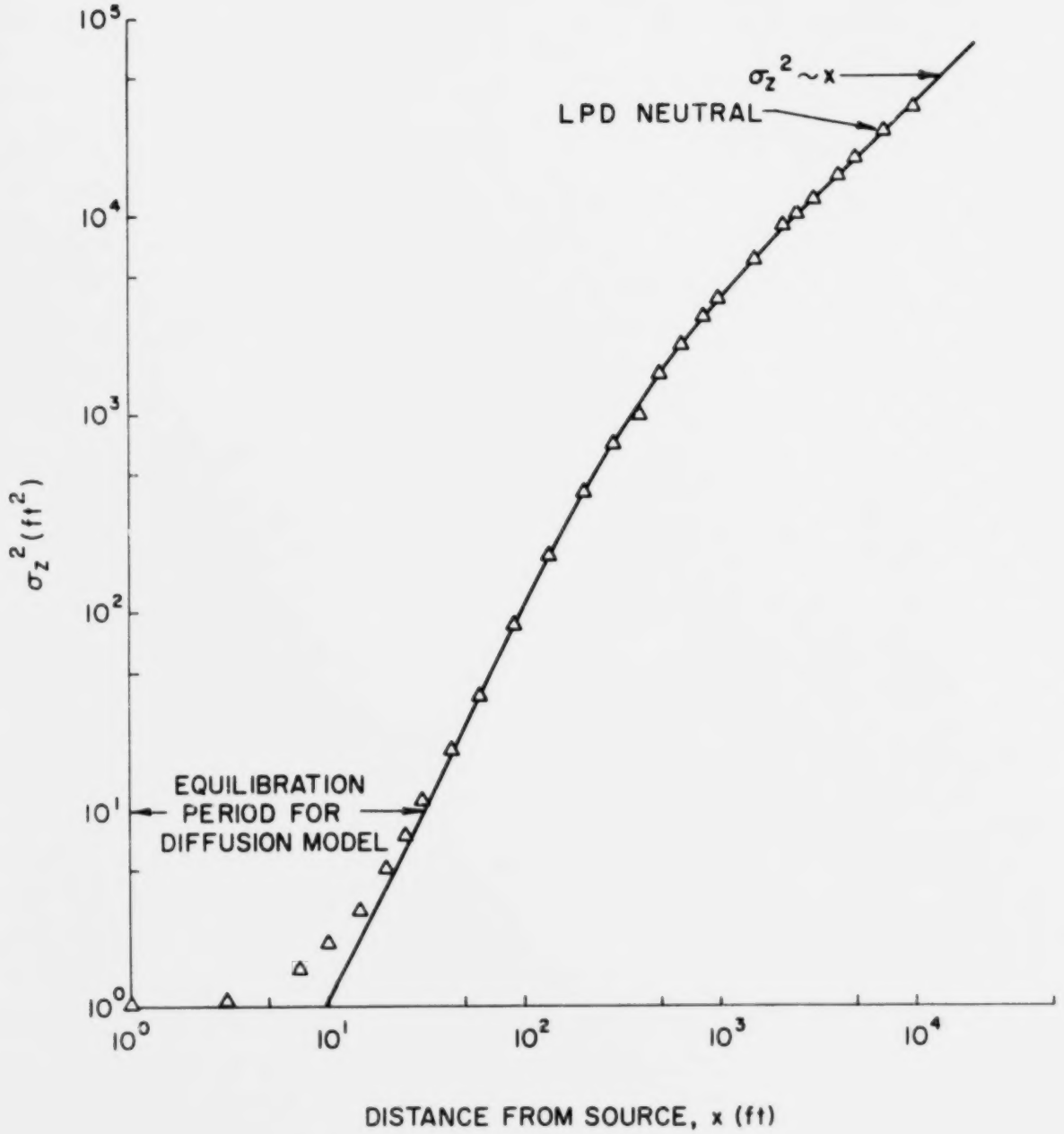

Figure 4. Variance of the vertical distribution of concentration σ_z^2 for the neutral case.

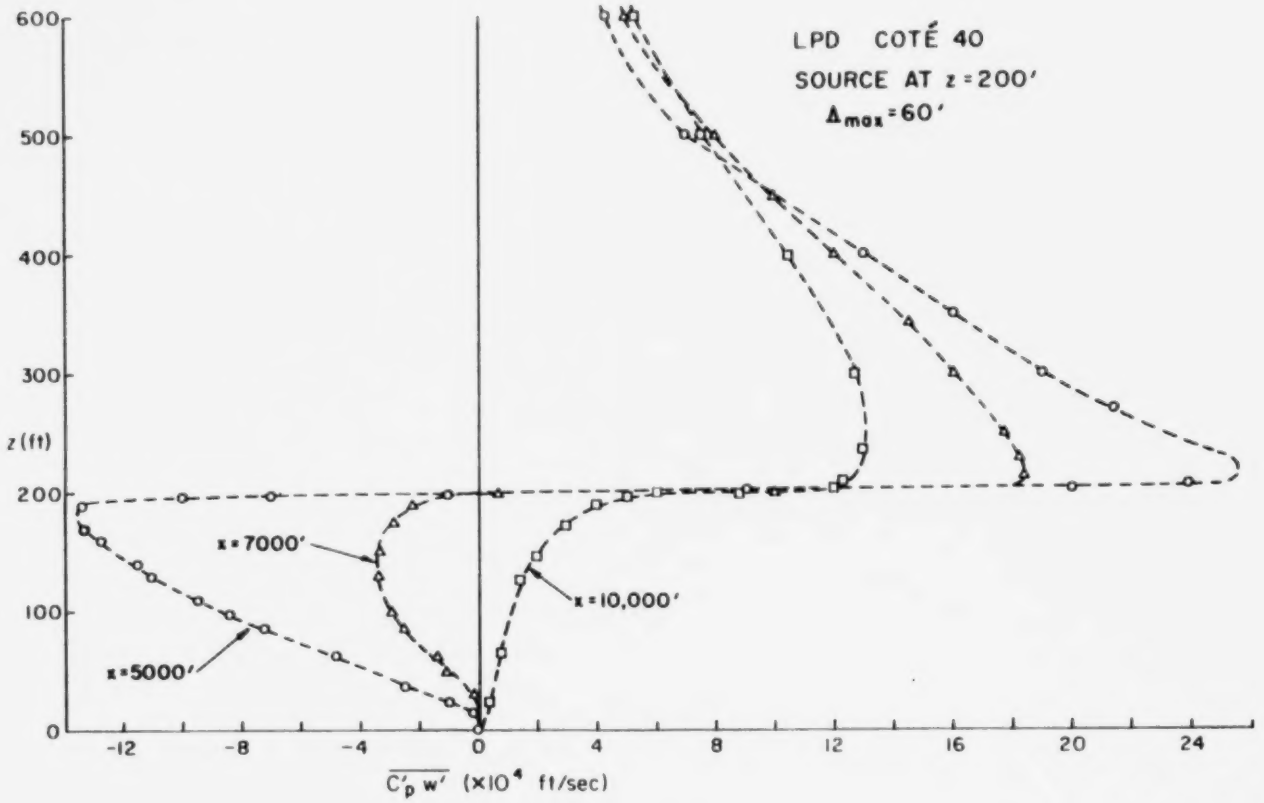

Figure 5. Profiles of predicted vertical turbulent flux of matter associated with concentration profiles shown in Figure 3.

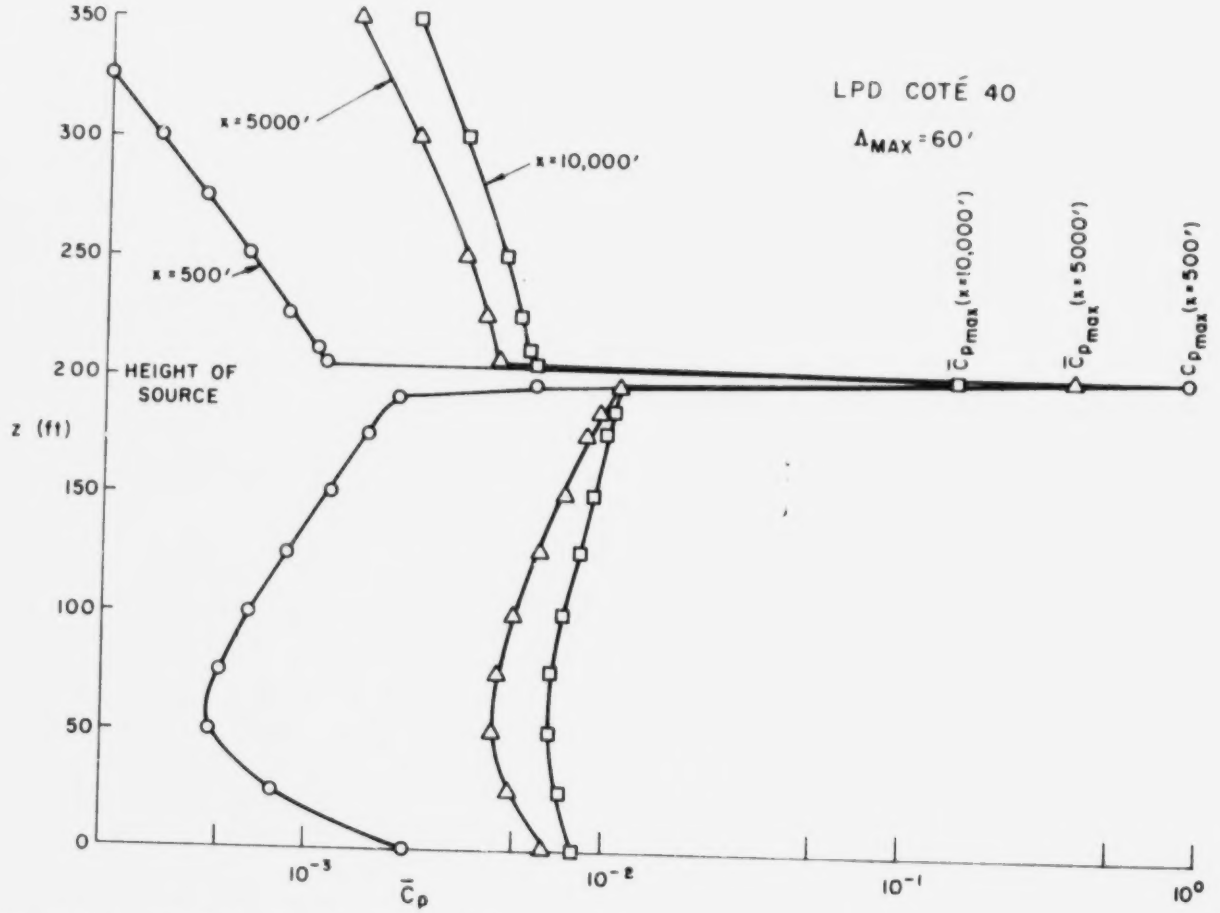

Figure 6. Vertical profiles of concentration at 500, 5000, and 10,000 feet downwind from a continuous crosswind source located at 200 feet above the surface in the stably stratified atmosphere.

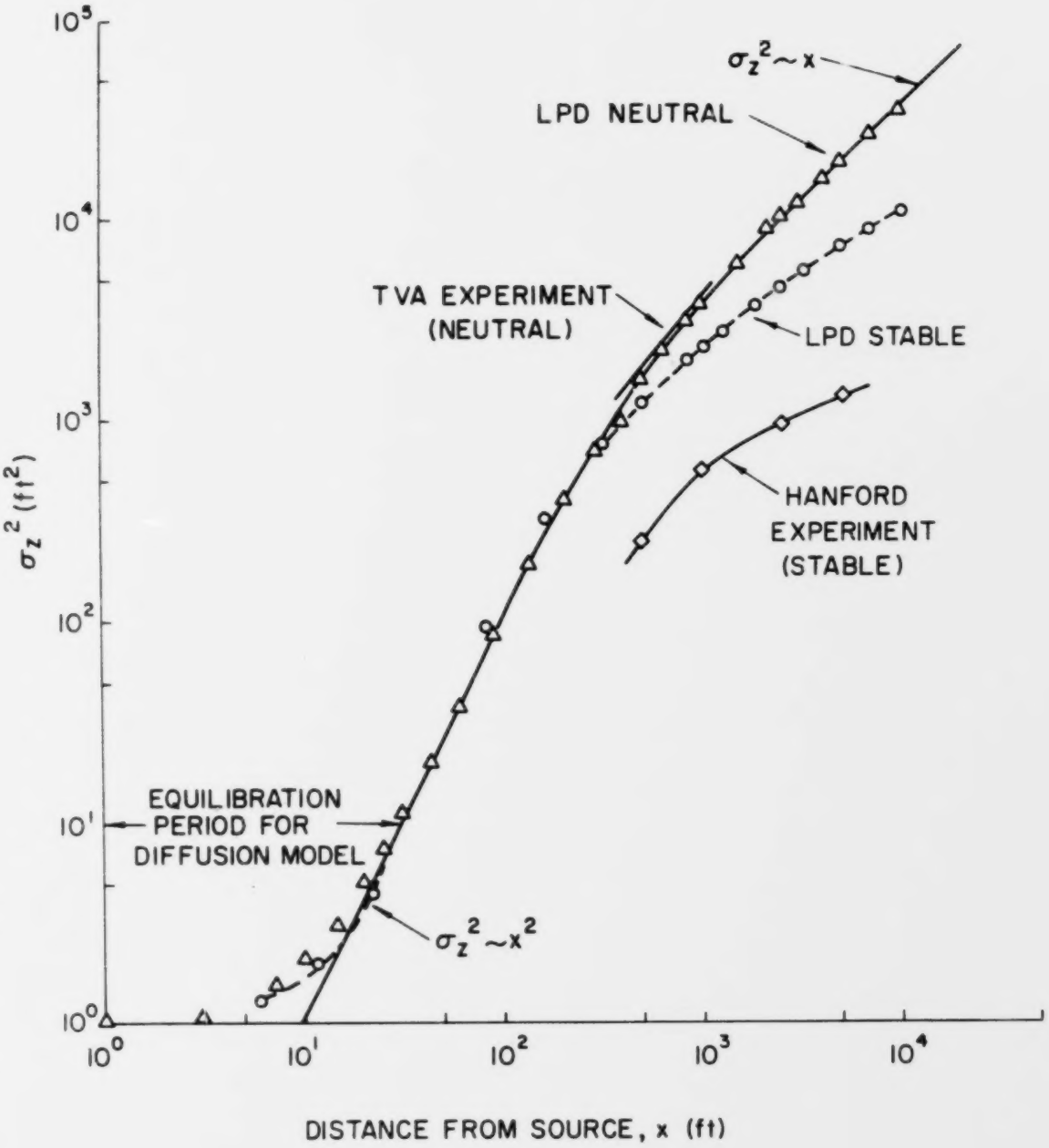

Figure 7. Variance of the vertical concentration distribution σ_z^2 for both the stable and the neutral cases, and comparison with experimental measurements.

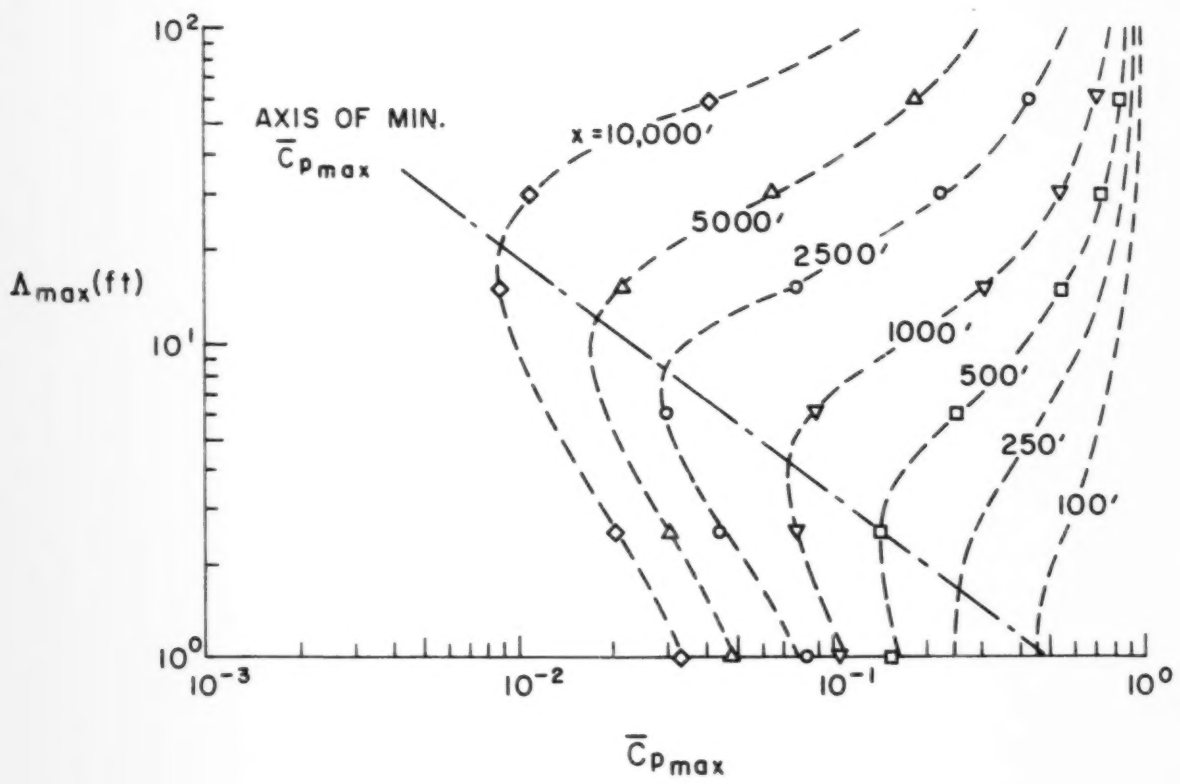

Figure 8. Summary of LPD predicted values of $\bar{C}_{p_{max}}$, the axial concentration, as a function of constant Λ_{max} and distance x (neutral atmosphere).

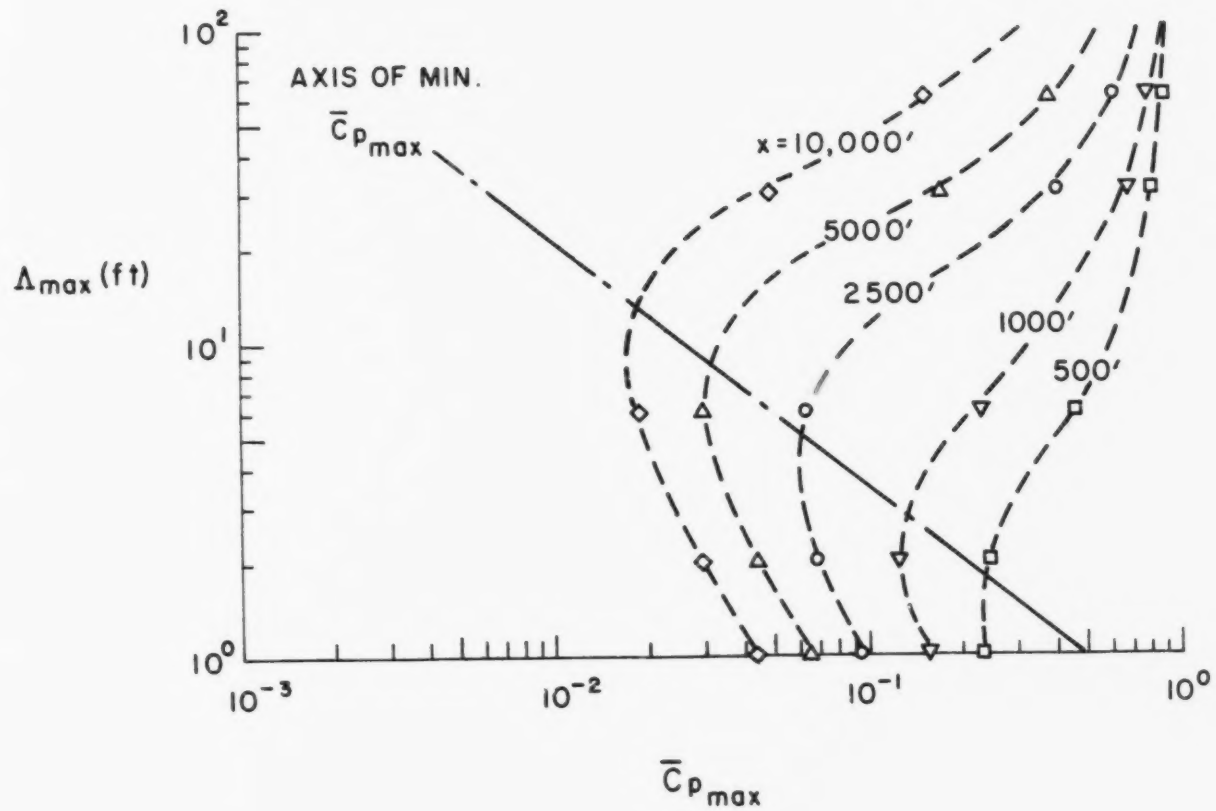

Figure 9. Summary of LPD predicted values of $\bar{C}_{p_{max}}$, the axial concentration, as a function of constant Λ_{max} and distance x (stable atmosphere).

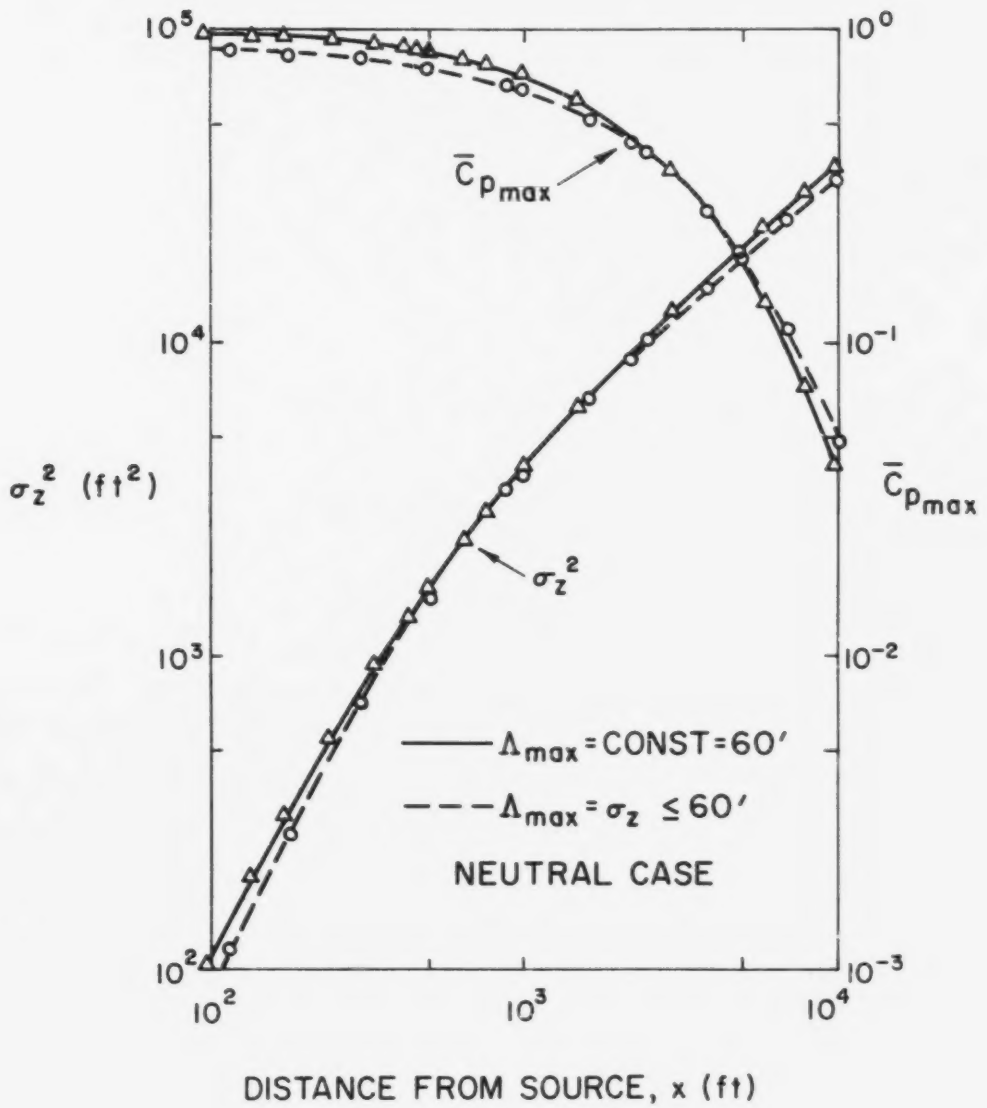

Figure 10. Comparison of predicted σ_z^2 and $\bar{C}_{p_{max}}$ when $\Lambda_{max} = \sigma_z \leq 60$ feet for the neutral case.

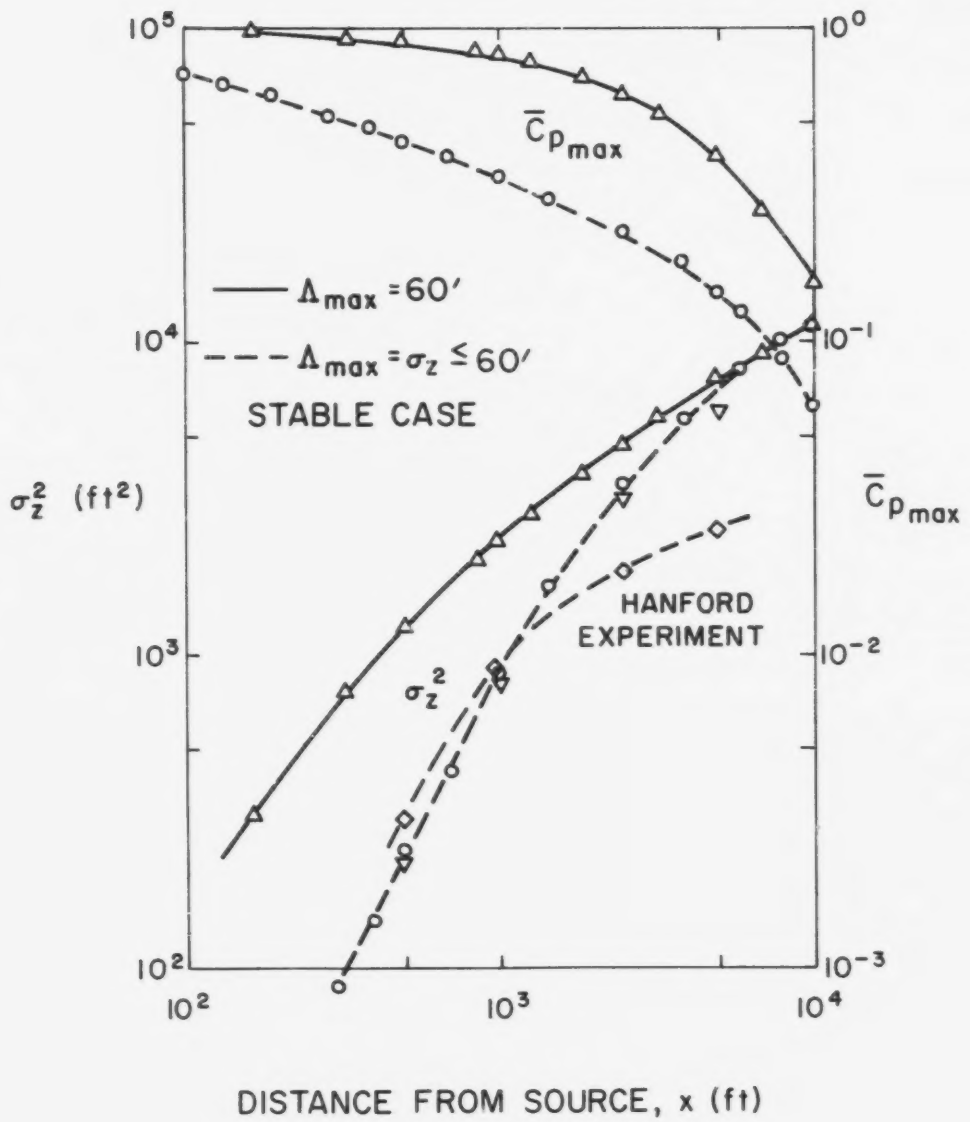

Figure 11. Comparison of predicted σ_z^2 and $\bar{C}_{p_{max}}$ when $\Lambda_{max} = \sigma_z \leq 60$ feet for the stable case.

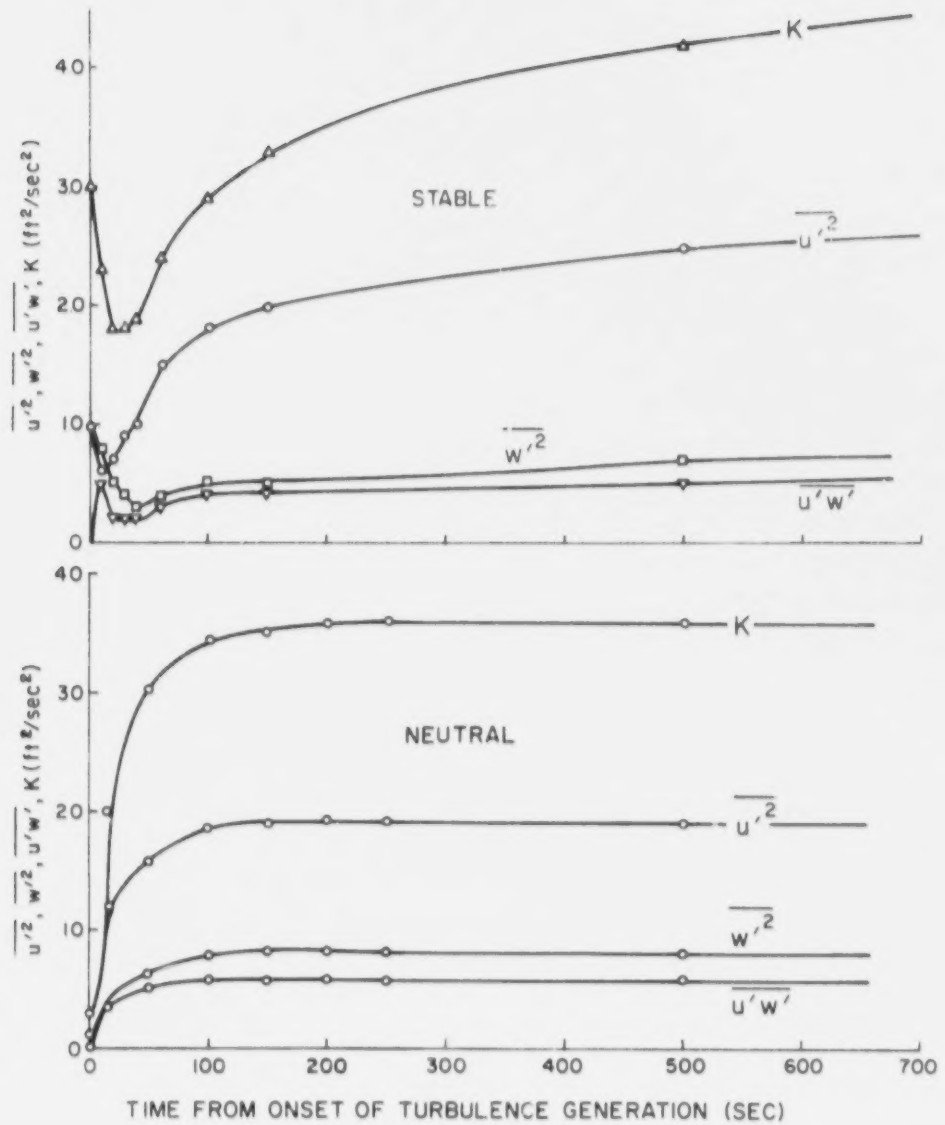

Figure 12. Time history of invariant model calculations of turbulence parameters (maxima of $\overline{u'^2}$, $\overline{w'^2}$, $K = \overline{u'^2}+\overline{v'^2}+\overline{w'^2}$, and $\overline{u'w'}$) showing time required for these parameters to come to equilibrium in neutral and stable atmospheres.

APPENDIX A

Theoretical Study of the Generation of Acceptable Clean Air Turbulence

53

Reprinted from AIAA JOURNAL, Vol. 10, No. 2, February 1972, pp. 162-170
Copyright, 1972, by the American Institute of Aeronautics and Astronautics, and reprinted by permission of the copyright owner

A Theoretical Study of the Generation of Atmospheric-Clear Air Turbulence

COLEMAN DU P. DONALDSON,* ROGER D. SULLIVAN,† AND HAROLD ROSENBAUM‡
Aeronautical Research Associates of Princeton Inc., Princeton, N.J.

This paper concerns a numerical study of the time history of the growth and decay of turbulence in the atmosphere. The study was motivated by a desire to better understand the behaviour of shear-generated turbulence in the Earth's atmosphere—the problem of clear air turbulence (CAT). The variant modeling technique is used to derive a closed set of equations that govern this phenomenon. The resulting set of equations allows, for the first time, a step-by-step numerical calculation of the growth of turbulent disturbances in atmospheric shear flows and the dependence of this growth on atmospheric instabilities.

Nomenclature§

A, B, C = const
a_1, a_2 = const
a, a_1, a_2, a_3, a_4 = const
c_p = specific heat at constant pressure
f = unknown function
g = acceleration due to gravity
g_{ij} = the metric tensor
K = $u^* u_\infty$
k = conductivity
k_T = eddy conductivity
l = Prandtl's mixing length
p = pressure
q = $K^{1/2}$ or $u^* u_\infty$
q_i = heat-flow vector
Re_λ = $\rho \lambda q / \mu$
T = temperature
t = time
u, v, w = x_1, x_2, and x_3 components of velocity
u_i = velocity vector
X = body force
x, y, z = Cartesian coordinates
x_j = general coordinate system
δ = boundary-layer thickness or scale of mean motion
δ_j^i = Kronecker delta
ε_{ij} = $u_{i,j} + u_{j,i}$
η = function defined in Eq. (66)
λ, Λ = scalar measures of length
μ, μ^* = first and second coefficients of viscosity
μ_T = eddy viscosity
ξ = function defined in Eq. (64)
ρ = density
σ = $(1/\rho_0)(\partial p_0/\partial z)$
τ_{ij} = stress tensor
ϕ = gravitational potential
ω = $2[(\omega_1 E_{1i} \omega_1 E_{1i}) + (\omega_2 E_{2i} \omega_2 E_{2i})]^{1/2}$

Subscript

0 = equilibrium conditions of the atmosphere

Superscripts

′ = departure from equilibrium
¯ = mean
″ = departure from the mean

Presented as Paper 70-55 at the AIAA 8th Aerospace Sciences Meeting, New York, January 19-21, 1970; submitted May 4, 1971; revision received August 23, 1971. This research was supported by NASA under Contract NASW-1868.

Index categories: Atmospheric, Space, and Oceanographic Science; Jets, Wakes, and Viscid-Inviscid Flow Interactions.

* President and Senior Consultant. Associate Fellow AIAA.

† Vice President and Consultant. Member AIAA.

‡ Associate Consultant, presently Senior Consulting Scientist, Avco Systems Division, Avco Corporation, Wilmington, Mass. Member AIAA.

§ The notation of general tensor analysis is used. In particular, the summation convention is implied, and a comma preceding a subscript indicates partial differentiation.

Introduction

FOR many years, those engaged in the study of turbulent motions have made use of the concepts of eddy viscosity and eddy conductivity to enable them to calculate the conduction of momentum and heat in these motions. In an incompressible medium to which these notions have been extensively applied, the eddy-conductivity concept relates the turbulent flux of momentum and heat to the gradient of the mean velocity and temperature fields according to

$$\tau_{ij} = \mu(u_{i,j} + u_{j,i}) - \rho\langle u_i u_j\rangle = (\mu + \mu_T)(u_{i,j} + u_{j,i}) \tag{1}$$

and

$$q_i = kI_{,i} - \rho c_p\langle u_i I\rangle = (k + k_T)I_{,i} \tag{2}$$

The eddy viscosity μ_T and the eddy diffusivity k_T in these expressions have, in the past, been determined either by resort to experiment or, more indirectly, from physical arguments which determined some basic and perhaps simpler parameters which could in turn be evaluated experimentally. The latter method has, in general, been preferred because of the hope that such parameters might have some simple general relationships by which they could be determined for a large class of flows. Of course, both these methods fail if τ_{ij} or q_i are not zero when $u_{i,j} + u_{j,i}$ and $I_{,i}$ vanish.

In view of the fact that the tensor $\langle u_i u_j\rangle$ and the vector $\langle u_i I\rangle$ both have dynamics of their own quite apart from (although related to) the dynamics of the mean fields u_i and I, the concept of eddy transport has been remarkably successful over the years in dealing with so many engineering problems. The explanation for this success lies in the fact that the dynamics of the turbulence is fast enough relative to the dynamics of the mean flow in many cases so that the turbulent correlations $\langle u_i u_j\rangle$ and $\langle u_i I\rangle$ are able to "track" the development of the mean motion. This is certainly true of developed pipe flows where the derivatives of all mean quantities, except the static pressure, with respect to streamwise position are zero.

On the other hand, a number of turbulent flows of interest exist in nature for which the turbulent correlations are not able to track the changes in the mean field u_i and I. In such flows, the dynamics of the turbulence is important, and the concept of eddy transport in any simple form is not a sufficiently powerful tool with which to study the motion.

As will be seen in what follows, the motion of the atmosphere is an example of such a flow. For this reason, a more powerful approach must be used — one which actually keeps track in some way of the dynamics of the turbulent correlations such as $\langle u_i u_j\rangle$ and $\langle u_i I\rangle$.

Within the past few years, a method has been developed by the senior author of this paper and his collaborators[1,2] which will, when it has been fully developed, permit one to calculate, with some degree of precision, the motion of strongly sheared turbulent layers. The method, which is called the method of invariant modeling, has been applied with some success to the calculation of incompressible turbulent boundary layers and to the decay of an isolated vortex. In this paper, we present the results of an initial application of the method to the calculation of atmospheric motions.

Brief Description of the Method of Invariant Modeling

It is beyond the scope of this paper to present a complete description of the method of invariant modeling. However, we give, in this section, a brief outline of the method, as well as a short discussion of its relationship to the mixing length model of turbulent transport proposed by Prandtl.[3]

Consider the motion of an incompressible medium which is governed by the Navier-Stokes equations so that the momentum equation may be written

$$\partial(\rho u_i)/\partial t + (\rho u_i u_j)_{,j} = -p_{,i} + \tau_{ij,j} \tag{3}$$

where

$$\tau_{ij} = \mu(u_{i,j} + u_{j,i}) \tag{4}$$

If we write the velocity vector u_i and the pressure as the sum of a mean part and a fluctuating part whose time average is zero, i.e., $u_i = u_i + u_i'$ and $p = p + p'$ with $u_i' = p' = 0$, Eq. (3) can be written, after time-averaging, as

$$\frac{\partial}{\partial t}(\rho u_i) + (\rho u_i u_j)_{,j} = -p_{,i} + (\tau_{ij}' - \rho\langle u_i' u_j'\rangle)_{,j} \tag{5}$$

This is the turbulent momentum equation derived by Reynolds.

To solve this equation we need to know the Reynolds stress tensor $-\rho\langle u_i' u_j'\rangle$. If the turbulent correlations can track the mean motion in the sense discussed in the previous section, we can assume that this tensor can be expressed in terms of the mean velocity field u.

Prandtl accomplished this for the case of a simple boundary-layer flow by means of a physical argument[3] and obtained the well-known result

$$\rho\langle u'v'\rangle = \rho l^2|u_{,y}|u_{,y} \tag{6}$$

where l (the "mixing length") is a scale parameter identified in the argument with a characteristic size of the turbulent motion.

We can obtain this result in another way. We ask whether one can write the tensor $\langle u_i' u_j'\rangle$ in terms of the mean motion u. The expression chosen must exhibit the symmetric-tensor character of $\langle u_i' u_j'\rangle$, must be dimensionally correct, must be invariant under a general transformation of coordinates, as well as under a Galilean transformation, and must not be such as to upset any of the general conservation laws. Since

$$\epsilon_{ij} = u_{i,j} + u_{j,i} \tag{7}$$

has the required symmetry and satisfies the invariance conditions, one might write

$$-\rho\langle u_i' u_j'\rangle = f(u_k)(u_{i,j} + u_{j,i}) \tag{8}$$

where $f(u_k)$ must be a scalar and must be such that the dimensions of the resulting expression are correct. Two simple choices for $f(u_k)$ have the required Galilean invariance. They are

$$f_1(u_k) = \Lambda^2 u_{m,m} \tag{9}$$

and

$$f_2(u_k) = \Lambda^2(\epsilon_{mn}\epsilon^{mn})^{1/2} \tag{10}$$

In these expressions, Λ is a scalar measure of length. The first expression above is zero by virtue of continuity, so we choose the second expression [Eq. (10)] so that

$$-\rho\langle u_i' u_j'\rangle = \Lambda^2(\epsilon_{mn}\epsilon^{mn})^{1/2}(u_{i,j} + u_{j,i}) \tag{11}$$

If the formula given above is reduced to the situation of a simple shear layer $u = u(y)$ with $v = w = 0$, one obtains

$$-\rho\langle u'v'\rangle = (2)^{1/2}\Lambda^2|u_{,y}|u_{,y} \tag{12}$$

which is essentially Prandtl's result. We conclude, therefore, that Eq. (11) represents a general form of Prandtl's mixing length expression for the Reynolds stress. We might expect such a result to hold provided the mean flow was such that the dynamics of the turbulence could track the mean motion. We also expect the scale parameter Λ to be related to the scale of the mean motion.

Suppose now we wish to generalize this idea to the case where the dynamics of the turbulence must be considered. We can write the equation for the Reynolds stress, namely,

$$\frac{\partial}{\partial t}(\rho\langle u_i' u_j'\rangle) + \rho u^m\langle u_i' u_j'\rangle_{,m} = -\rho\langle u^m u_i' u_{j,m}\rangle - \rho\langle u^m u_j' u_{i,m}\rangle$$
$$-\rho\langle u^m u_i' u_j'\rangle_{,m} - \langle u_i' p'\rangle_{,j} - \langle u_j' p'\rangle_{,i} + p\langle u_{i,j}' + u_{j,i}'\rangle$$
$$+\mu\langle u^m{}_{,m} u_i' u_j'\rangle_{,m} - 2\mu\langle u^m{}_{,m} u_{i,n}' u_{j,n}'\rangle \tag{13}$$

and we note that correlations other than the second-order correlation $\langle u_i' u_k'\rangle$ itself appear in the equation.

If we wish to close the set of equations to be solved with no more equations than those describing u_i and $\langle u_i' u_j'\rangle$, we must express these extra terms through the use of quantities for which we already have equations. In the method of invariant modeling, we do this by choosing expressions for these terms based on the second-order correlations themselves which satisfy the general rules for modeling set forth above in the discussion of Prandtl's

55

mixing length. When this procedure is followed, one can actually obtain only a few models which satisfy the rules set down and which are reasonably simple expressions representing straightforward physical principles. The following model has been investigated in some detail:

$$\overline{u''^m u_i u_j} = \Lambda\rho\left[\overline{u''^m u_i u_{j,k}} + \overline{u''^m u_{i,k} u_j} + \overline{u''^m u_k u_{i,j}}\right] \quad (14)$$

$$\overline{p u_{i,j}} + \overline{u_i p_{,j}} = \tau\rho\Lambda\left[\overline{u_i (k, j)} - \overline{u_i u_j}\right] \quad (15)$$

$$\overline{u''^m u_{m,k} u_k} = \overline{u_i u_{i,k}} \quad (16)$$

$$\overline{u_i p} = p\Lambda\rho\overline{u''^m u_{i,m}} \quad (17)$$

In this model there are two scale parameters Λ and τ. They are related in concept to the integral and microscales of the turbulence. In our work, we have taken them to be related to each other by the expression

$$\tau^2 = \Lambda^2 (c_1 + c_2 R_{c_3}) \quad (18)$$

Equation (18) has been used by Glushko[4] and by Beckwith and Bushnell[5] when modeling the turbulent kinetic energy equation obtained from Eq. (1) by contraction.

In applying the model to the incompressible boundary layer on a flat plate, we assume that in the outer regions of the boundary layer the scale Λ is a constant fraction of the boundary-layer thickness δ:

$$\Lambda = c_3\delta \quad (19)$$

Near the surface in the boundary layer we assume that Λ is proportional to the distance normal to the surface, i.e.,

$$\Lambda = c_4 z \quad (20)$$

for $z > 0$. An examination of the boundary conditions at $z = 0$ shows, however, that the constant c_4 must be related to c_3 so that only three parameters, c_1, c_2, and c_3, must be determined from experimental data.

To see the relationship between c_3 and c_4, we note that at the surface we must have

$$\tau^2 = \overline{u_i u_{i,z}} + \overline{u_i^2} = 2\overline{u_i u_{i,z}} + \tau^2 \quad (21)$$

Now $\overline{u_i u_{i,z}}$ must be zero at $z = 0$, and, since $\overline{u_i u_{i,z}}$ represents the flux of $\overline{u_i u_i}$ through the surface $z = 0$ by viscous diffusion, which is not physically possible, we must have $\overline{u_i u_{i,z}} = 0$ at $z = 0$. Thus we have near $z = 0$

$$\overline{u_i u_{i,z}} = \overline{u_1 u_{1,z}} + \overline{u_2 u_{2,z}} + \cdots \quad (22)$$

Substituting Eq. (22) into Eq. (21) results in

$$\tau^2 = 2\overline{u_1 u_{1,z}} + \overline{u_2 u_{2,z}} + \cdots + 1 = 2\overline{u_1 u_{1,z}} + 6\overline{u_1 u_{1,z}} \quad (23)$$

or (unless $\overline{u_1 u_{1,z}} = 0$ for $z > 0$)

$$\tau = 1 \quad (24)$$

Since $R_{c_3} > 0$, Eq. (18) can be written

$$\tau^2 = \Lambda^2 c_1 \quad (25)$$

for small z. Thus, from Eqs. (20) and (24) we get

$$1^2 = c_4^2 z^2 c_1 \quad (26)$$

or

$$c_4 = \frac{1}{z\sqrt{c_1}} \quad (27)$$

We have applied this model to the turbulent boundary layer on a flat plate and have compared the results with the standard data on such flows[6] in an attempt to determine the best values of c_1, c_2, and c_3. When this was originally done, the following values for the parameters were found:

$$c_1 = 2.5, \quad c_2 = 0.125, \quad c_3 = 0.064 \quad (28)$$

Subsequently, an error was found in the computer program so that the values of the parameters given previously are not now considered to be those that will give an optimum fit to existing experimental data. They are, however, not far different from the optimum values. In the work that will be presented in the remainder of this paper, the values given in Eq. (28) were used. We believe, therefore, that the results we shall present are correct as to the general behavior of the atmosphere, although the exact numerical values of the various quantities computed will be altered somewhat when the new "optimum" values of the parameters that are presently being generated are inserted into our atmospheric programs.

Equations of Atmospheric Motion

Since the variation of density with altitude plays an important part in atmospheric motion, the equations above do not apply. The appropriate equations are generally written in terms of the departure of the various physical quantities, I, p, and u_i, from the values they would have in an atmosphere at rest, namely, I_∞, ρ_∞, p_∞ (which are functions of altitude only) and $u_{i_\infty} = 0$. Thus, we define

$$I = I - I_\infty, \quad \bar{\rho} = \rho - \rho_\infty, \quad p = p - p_\infty \text{ and } u_i = u_{i_\infty} \quad (29)$$

These quantities, in turn, are split into their mean and fluctuating parts, so that, for the rest of this paper, I stands for the mean of I and $I = I - I$. The other variables are treated the same way.

With the assumption of small departures from equilibrium, the equations for the turbulent atmosphere are

$$\rho_\infty u_i(\partial I/\partial t) + \rho_\infty u^m u_i I_{,m} = -p_{,i} + \{\mu a^{m_\infty} u_{i,m} + u_{m,i}\} + \mu^* u_{m,m}^{m_\infty} - \rho_\infty u^m u_i\}_{,i} + \rho_\infty I_\infty \partial I/\partial z_i \quad (30)$$

$$\partial\rho_\infty I/\partial t + \rho_\infty u^m I_{,m} = \alpha a^{m_\infty} I_{,m} - \rho_\infty u^i I^{-1}{}_{,i} \quad (31)$$

$$u_{,i}^1 = \alpha a^{i_\infty}\rho_\infty b_{\infty,i} \quad (32)$$

$$u_{,i}^1 = \alpha a^{i_\infty}\rho_\infty b_{\infty,i} \quad (33)$$

$$\rho_\infty^{-1} u_i u_j = I + \rho_\infty u^m u_i u_{j,m} = \rho_\infty u^m u_j u_{i,m} + \rho_\infty u^m u_i u_{j,m} - \rho_\infty u^m u_i u_j{}_{,m} - u_i p_{,j} - u_j p_{,i} + p(u_{i,j} + u_{j,i}) + \mu a^{m_\infty} u_i u_{j,m} - 2\mu a^{m_\infty} u_{i,m} u_{j,m} + (\mu + \mu^*)\{u^m u_i \partial\rho_{\infty,m}/\partial z_j + u^m u_j \partial\rho_{\infty,m}/\partial z_i + \rho_{\infty,m}\partial^2 u_i u_j^{m_\infty} + u_j u_{i,z}^{m_\infty} + 1\} + \rho_\infty I_\infty b(\phi_{,i} u_j I^{-1} + \phi_{,j} u_i I^{-1}) \quad (34)$$

$$\{\rho_\infty^{-1} u_i I^{-1} + I\} + \rho_\infty u^m u_i I^{-1}{}_{,m} = \rho_\infty u^m u_i I_{,m} + \rho_\infty u^m I u_{i,m} - (\rho_\infty u^m u_i I^{-1})_{,m} - p I^{-1}{}_{,i} + p I_{,i} + \mu a^{m_\infty} u_i I^{-1}{}_{,m} - 2\mu a^{m_\infty} u_{i,m} I_{,m} + (\mu + \mu^*)\{u^m I \partial\rho_{\infty,m}/\partial z_i + (I u_i^{m_\infty} + \rho_{\infty,m}\rho_\infty)\} + \rho_\infty I_\infty b\phi_{,i} I^{-2} \quad (35)$$

$$\{\rho_\infty^{-1} I^{-2} + I\} + \rho_\infty u^m I^{-2}{}_{,m} = 2\rho_\infty u^m I^{-1} I_{,m} + \rho_\infty u^m I^{-2}{}_{,m} + \alpha a^{m_\infty} I^{-2}{}_{,m} - 2\mu a^{m_\infty} I_{,m} I_{,m} \quad (36)$$

In these equations, we have taken the Prandtl number, $\mu c_p/k$, equal to one, but we have not made the usual assumption that $u_{,i}^1 = 0$ as is done in Ref. 7 and which, in general, restricts the motions which may be studied to those which are small in scale compared to the scale of the atmosphere.

If Eqs. (34–36) are studied, one sees that, if the terms containing $\rho_\infty^{-1}\rho_{\infty,i}$ are dropped, the invariant modeling we have already carried out for boundary-layer flows may be taken over without the introduction of new parameters to the calculation of atmospheric motions. If we keep the terms containing $\rho_\infty^{-1}\rho_{\infty,i}$, we find that the modeling is changed slightly so as to satisfy the conservation law given in Eq. (33). The important point, however, is that no new parameters are introduced and the three parameters c_1, c_2, and c_3 discussed in the previous section are sufficient to determine the motion. We use the following modeling:

$$\overline{u''^m u_i u_j} = \Lambda\rho\left[\overline{u''^m u_i u_{j,m}} + \overline{u''^m u_{i,m} u_j} + \overline{u''^m u_m u_{i,j}}\right] \quad (37)$$

$$\overline{u''^m u_i I} = \Lambda\rho\left[\overline{u''^m u_i I_{,m}} + \overline{u''^m I u_{i,m}}\right] \quad (38)$$

$$\overline{u''^m I^{-1}} = \Lambda\rho\overline{u''^m I^{-1}{}_{,m}} \quad (39)$$

$$\overline{u''^m u_{i,m} u_{j,n}} = \overline{u_i u_{j,z}} + \tau^2 \quad (40)$$

$$\overline{u''^m u_{i,m} I_{,n}} = \overline{u_i I^{-1}{}_{,z}} \quad (41)$$

$$\overline{u''^m I_{,m} I_{,n}} = \overline{I^{-1}{}_{,z}} \quad (42)$$

$$\overline{u_i p} = -\rho_\infty\Lambda\rho\overline{u''^m u_{i,m}} \quad (43)$$

$$\overline{p I^{-1}} = -\rho_\infty\Lambda\rho\overline{u''^m I^{-1}{}_{,m}} \quad (44)$$

56

$$p(u_i + u_i') = (\rho_0 q \Lambda/\varepsilon)[a_{ij}(K,3) - u_i u_j] - u_i p - \rho_{0,j}\rho_0^{-1} u_i p - \rho_{0,i}\rho_0^{-1} u_j p \quad (45)$$

$$p I = (\rho_0 q \Lambda/\varepsilon) I - u_j I \quad (46)$$

$$u_i u_j^m = -a^m u_i - \rho_{0,j}\rho_0^{-1} u_i \quad (47)$$

$$I u_j^m = -a^m I - \rho_{0,j}\rho_0^{-1} I \quad (48)$$

Equations (30–36), together with the modelings given above, now constitute the equations with which we propose to study the nature of turbulence generation in the atmosphere as a result of winds and thermal instabilities. Of course, this can only be done for very simple motions for which we will be able to identify the scale of the mean fields of u_i and I. In what follows, we will apply the equations given in this section to a particularly simple example of atmospheric motion with the idea of demonstrating some of the behavior of atmospheric shear layers as indicated by our equations.

A Simple Case of Atmospheric Shear

In order to study the nature of atmospheric motion as described by the equations given above, we have selected what we consider to be the simplest motion that can give meaningful results. We consider an atmosphere in which the motion $u(z,t)$ in Cartesian coordinates (x,y,z) is such that $u = u(z,t)$ and $v = w = 0$. Thus, we assume that the mean motion consists of only one component of velocity. That component of velocity is parallel to the ground and is only a function of time and altitude. In such a motion, symmetry requires that the correlations $\overline{uI}$, $\overline{u\varepsilon}$, and $\overline{uw}$ be zero. To gain this amount of simplicity in the motion, it is necessary to invent a body force $X(z,t)$ which starts the motion. Actually, there is no such real force acting on the atmosphere but rather the atmosphere is driven by pressure and Coriolis forces. These forces, however, produce a far more complicated motion in the large than the one we have chosen. At the very least, one must, in such cases, consider a motion of the form $u(z,t)$ and $w(z,t)$. Nevertheless, these real motions can resemble locally the simple motions we shall study here. We believe that the essential features of atmospheric-turbulence production will be demonstrated by our somewhat fictitious atmospheric model while retaining a relatively simple set of governing equations. For the motion we have just described, the equations given in the previous section become

$$\rho_0 \partial u/\partial t = (\mu + \mu^*)\partial^2 u/\partial z^2 - \partial[\rho_0 \overline{uw} + \tau_{xz}]/\partial z + X(z,t) \quad (49)$$

$$\rho_0 \partial I/\partial t = (\mu + \mu^*)\partial^2 I/\partial z^2 - \partial[\rho_0 \overline{wI} + \tau_{xz}]/\partial z \quad (50)$$

$$\partial p/\partial z = -\varepsilon/a^2 - \rho_0 \overline{ww}_{,z} + \tau_{zz}/\rho_0 a^2 I \quad (51)$$

$$\partial \overline{uu}/\partial t = -2\overline{uw}\,\partial u/\partial z - \partial/\partial z\left(\rho_0 q \Lambda \partial \overline{uu}/\partial z\right) - \frac{q}{\Lambda}\left(\overline{uu} - \frac{K}{3}\right) + \frac{\mu + \mu^*}{\rho_0}\partial^2 \overline{uu} - \frac{2\mu - \mu^*}{\rho_0}\frac{\overline{uu}}{z^2} \quad (52)$$

$$\partial K/\partial t = -\partial/\partial z\left(\rho_0 q \Lambda \partial K/\partial z\right) - \frac{q}{\Lambda}\left(\varepsilon - \frac{K}{3}\right) + \frac{\mu + \mu^*}{\rho_0}\partial^2 K - \frac{2\mu - \mu^*}{\rho_0}\frac{K}{z^2} \quad (53)$$

$$\partial \overline{ww}/\partial t = -\frac{3}{\rho_0}\partial/\partial z\left(\rho_0 q \Lambda \partial \overline{ww}/\partial z\right) - \frac{q}{\Lambda}\left(\overline{ww} - \frac{K}{3}\right) + 2\pi \Lambda q \partial \overline{ww}/\partial z + \frac{2}{\rho_0}\partial/\partial z\left(\rho_0 q \Lambda \partial \overline{ww}/\partial z\right) + \frac{\mu + \mu^*}{\rho_0}\partial^2 \overline{ww} - \frac{2\mu - \mu^*}{\rho_0}\frac{\overline{ww}}{z^2} + \frac{2\mu - \mu^*}{\rho_0}\left[\overline{ww} - \left(\frac{\varepsilon}{\rho_0} - \sigma^2\right)\right] + \frac{2q}{I_0}\overline{wI} \quad (54)$$

$$\partial \overline{uw}/\partial t = -\overline{uw}\,\partial u/\partial z - \overline{wI}\,\partial u/\partial z - \partial/\partial z\left(\rho_0 q \Lambda \partial \overline{uw}/\partial z\right) - \frac{q}{\Lambda}\overline{uw} + \sigma \Lambda q \partial^2 \overline{uw}/\partial z^2 + \frac{\mu + \mu^*}{\rho_0}\partial^2 \overline{uw} - \frac{2\mu - \mu^*}{\rho_0}\frac{\overline{uw}}{z^2} + \frac{2\mu - \mu^*}{\rho_0}\left[\overline{uw} - \left(\frac{\varepsilon}{\rho_0} - \sigma^2\right)\right] + \frac{q}{I_0}\overline{uI} \quad (55)$$

$$\partial \overline{uI}/\partial t = -\overline{uw}\,\partial I/\partial z - \overline{wI}\,\partial u/\partial z + \partial/\partial z\left(\rho_0 q \Lambda \partial \overline{uI}/\partial z\right) - \frac{q}{\Lambda}\overline{uI} + \frac{\mu + \mu^*}{\rho_0}\partial^2 \overline{uI} - \frac{2\mu - \mu^*}{\rho_0}\frac{\overline{uI}}{z^2} \quad (56)$$

$$\partial \overline{wI}/\partial t = -\overline{ww}\,\partial I/\partial z + 2\partial/\partial z\left(\rho_0 q \Lambda \partial \overline{wI}/\partial z\right) + \frac{1}{\rho_0}\partial/\partial z\left(\rho_0 q \Lambda \partial \overline{wI}/\partial z\right) - \frac{q}{\Lambda}\overline{wI} + \frac{\mu + \mu^*}{\rho_0}\partial^2 \overline{wI} - \frac{2\mu - \mu^*}{\rho_0}\frac{\overline{wI}}{z^2} + \frac{2\mu - \mu^*}{\rho_0}\left[\overline{wI} - \left(\frac{\varepsilon}{\rho_0} - \sigma^2\right)\right] + \frac{q}{I_0}\overline{I^2} \quad (57)$$

$$\partial \overline{I^2}/\partial t = -2\overline{wI}\,\partial I/\partial z + \frac{1}{\rho_0}\partial/\partial z\left(\rho_0 q \Lambda \partial \overline{I^2}/\partial z\right) + \frac{\mu + \mu^*}{\rho_0}\partial^2 \overline{I^2} - \frac{2\mu - \mu^*}{\rho_0}\left(\frac{\overline{I^2}}{z^2}\right) \quad (58)$$

From our previous work on invariant modeling, we will keep the following results

$$\sigma^2 = \Lambda^2(2.5 + 0.125 R_{EA}) \quad (59)$$

$$\Lambda = 0.064\delta \quad (60)$$

In this last equation, we will assume that δ is some appropriately chosen scale of the mean motion which will be akin to the boundary-layer thickness of our previous studies.

In the present study, we do not consider any interaction of the turbulence that is produced with the ground since we will, in general, be studying the generation of shear layers at altitude. However, if we were to do so, we would choose

$$\Lambda = (2.5)^{-1/2}\varepsilon \quad (61)$$

in the region from the ground to the point where

$$z = [0.064(2.5)^{-1/2}]\delta \quad (62)$$

Initial Computations

To date we have made only a few computations based on the scheme laid out in the preceding section. These initial computations represent the simplified cases which were used to check the program and are not meant to represent any particular physical situation. As may be seen by an examination of Eqs. (49–57), if we neglect the terms containing σ, which amounts to assuming the usual equations of atmospheric motion for which the scale of the motion is small compared to the scale of the atmosphere, and if we take, consistent with this assumption, ρ_0 equal to a constant, the solution of the equations will exhibit certain symmetries with respect to symmetric initial inputs that are useful in checking the program. The four problems we shall discuss are solutions of Eqs. (49–57) for the case when ρ_0 is constant.

The atmosphere is assumed to have initially a 4000-ft thick band of turbulence that is isotropic with $\overline{u^2} = \overline{v^2} = \overline{w^2} = 1$ (fps)^2. The band is centered at an altitude of 20,000 ft although the actual value of the altitude has no bearing on the problem due to the assumption that ρ_0 is constant. The initial sharp edges of the turbulent band are soon smoothed off by the action of the diffusion and dissipation terms of the equations. The atmosphere is initially at rest, i.e., at $t = 0$, $u = 0$. For a time, a body force acts on the atmosphere, creating a mean motion. The body force in the calculations we present here was taken to be of the form (Fig. 1)

$$X(z,t) = c(1 - z^2/\delta^2) \quad (63)$$

57

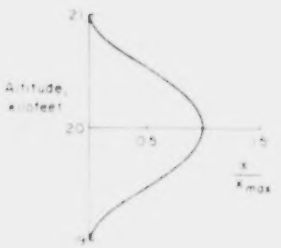

Fig. 1 Shape of the mean-velocity forcing function.

where

$$\zeta = (z - 20{,}000)/1000 \tag{64}$$

for

$$|\zeta| < 1 \tag{65}$$

In Eq. (64), z is an actual altitude in feet. Outside the region $|\zeta| < 1$, the driving force is taken to be zero. Thus, the forcing function is such that it produces a mean shear layer some 2000 ft thick. In the particular examples which we consider here, this forcing function is such that in the absence of any turbulence or viscosity the centerline velocity would increase to 30 fps in 3000 sec. After 3000 sec, it was assumed to vanish and the atmosphere left to dissipate the motion by turbulence and viscous diffusion.

Four cases of initial mean temperature distribution were considered (Fig. 2).

Case I: neutrally stable atmosphere $T(z,0) = 0$.

Case II: unstable-stable-unstable atmosphere given by $T(z,0) = (135.32)(2 - |\zeta|)^2$ for $|\zeta| < 2$ and zero elsewhere. Notice that this initial temperature is spread over 4000 ft rather than 2000 ft as was the case for the forcing function. The maximum temperature difference is 10 R.

Case III: stable-unstable-stable atmosphere given by $T(z,0) = -(135.32)(2 - |\zeta|)^2$ in the region $|\zeta| < 2$ and zero elsewhere.

Case IV: stable-unstable atmosphere given by $T(z,0) = 100(1 - \eta^2)^2$ where

$$\eta = \tfrac{1}{2}\zeta = (z - 20{,}000)/2000 \tag{66}$$

for $|\eta| < 1$ and zero elsewhere. This formula again gives a maximum temperature difference of 10 R.

The other initial conditions that have been used for these computations are

$$\overline{u'w'}(z,0) = 0; \quad \overline{w'T'}(z,0) = 0; \quad \text{and} \quad \overline{T'^2}(z,0) = 0$$

The scale Λ for all calculations was taken to be the length defined by 0.064 times the breadth of the mean shear layer as based on the distance between the points where the mean velocity falls to half its maximum value.

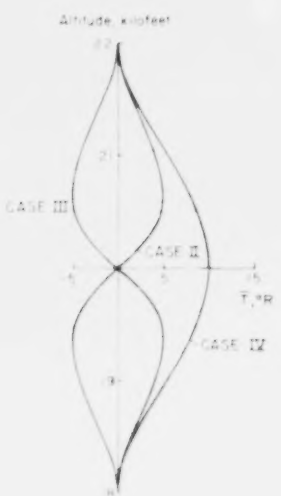

Fig. 2 Initial temperature profiles.

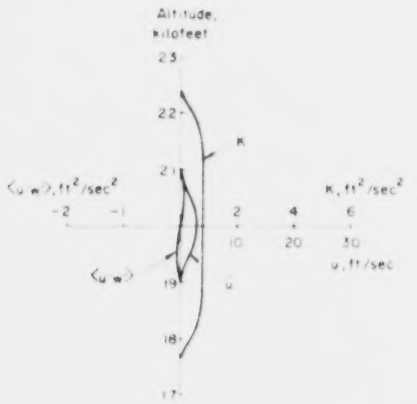

Fig. 3 $\bar{u}$, $\overline{u'w'}$, and K = $\overline{u'^2} + \overline{v'^2} + \overline{w'^2}$ for a neutrally stable atmosphere; Case I at 300 sec.

Results

Case I: Neutrally stable atmosphere

In Figs. 3, 4, and 5, we show the calculated values of the mean velocity $\bar{u}$, K = $\overline{u'^2} + \overline{v'^2} + \overline{w'^2}$, and $\overline{u'w'}$ for three times, 300, 3000, and 6000 sec, respectively. The first figure shows the very start of the development of the mean motion. At this time, very little turbulence has been created by the mean motion. Most of the turbulent energy that is seen is left over from the decaying initial turbulent layer. In Fig. 4, which shows the motion at the end of the application of the forcing function, the mean velocity is a maximum. The production of turbulent energy as a result of the deformation $\partial\bar{u}/\partial z$ is evident. The magnitudes of K and $\overline{u'w'}$ that are calculated are consistent with the results of tests on freejets in the laboratory. Figure 5 shows the motion after decay has set in. The mean velocity has spread, and the centerline value of K has started to fill in by diffusion.

Another picture of the development of this motion can be had by plotting the maxima of the various correlations determined at any time against time. This is done in Fig. 6. Here we see the initial decay of the turbulent layer with which we started, followed by the production of the various correlations as a result of the interaction between this turbulence and the mean flow. Once the forcing function ceases to increase the mean velocity, the jet that has been formed decays in the typical self-similar manner of laboratory jets.

Case II: Unstable-stable-unstable atmosphere

In Fig. 7, we show the mean-velocity profile at 3000 sec for the production of a shear layer in an unstable-stable-unstable

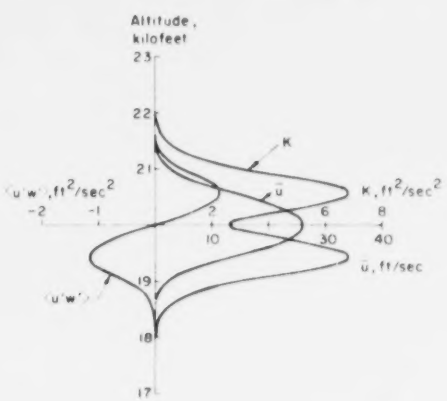

Fig. 4 $\bar{u}$, $\overline{u'w'}$, and K for Case I at 3000 sec.

58

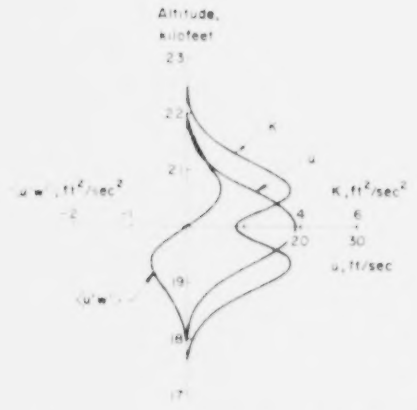

Fig. 5. u, $\overline{u'w'}$, and K for Case I at 6000 sec.

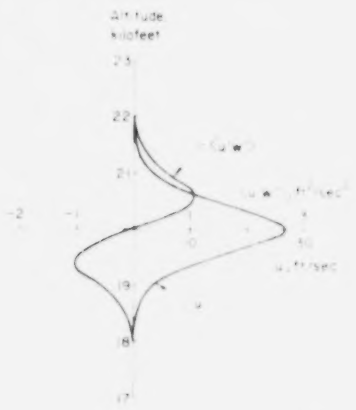

Fig. 7. u and $\overline{u'w'}$ for Case II at 3000 sec.

atmosphere. We note from a comparison of this figure with Fig. 4 (and the result is generally true) that at the maximum of the mean velocity, the mean velocity and shear $\partial u/\partial z$ are changed somewhat but not drastically by the effect of the temperature profile. As may be seen in Fig. 8, where we have plotted K and l^2 for both 300 and 3000 sec, the development of the turbulence is significantly altered. At small times, the contribution of the vertical component of velocity to the turbulent energy is large and is due to the basic thermal instability. The maximum value of K at this time is well outside the region of normal production by $\overline{u'w'}\,\partial u/\partial z$. As time progresses, however, the production of turbulent energy by $\overline{u'w'}\,\partial u/\partial z$ becomes large, and the maximum of K occurs near the maximum of $\overline{u'w'}\,\partial u/\partial z$ as may be seen from the K curve for 3000 sec.

In Fig. 9, we show the behavior of the heat-flux correlation $\overline{w'T'}$ and the mean temperature for times of 300 and 3000 sec. Here we note the very large values of $\overline{w'T'}$ in regions of $\partial T/\partial z > 0$ and the very small values of $\overline{w'T'}$ in regions of $\partial T/\partial z < 0$. The values of $\partial T/\partial z$ are not very different, and the level of turbulence K at times greater than 3000 sec cannot account for this difference. That is to say, none of the usual eddy diffusivity models could account for this behavior and the very persistent nature of the inversion that has been calculated here. A close inspection of the solution in the neighborhood of $z = 20000$ (the center of the inversion) indicates that at small times (t less than approximately 300 sec), the solution for $\overline{w'T'}$ is oscillatory. This strange behavior of the solution is not a quirk of the program or the modeling procedures that are used but is a result of the basic nature of the production equations when the atmosphere is stable, as will be discussed below.

In Fig. 10, we have again plotted the behavior of the maxima of the velocity correlations as a function of time. Note first the general production of turbulence by thermal instability at small times. Near the maximum of the mean velocity, the production of turbulence resembles that of the neutral atmosphere. Once the forcing function disappears, the mean motion dissipates and the thermal instabilities in the outer regions of the motion take over. In this case they just about balance dissipation as time proceeds. This is due to the increase in the dissipation scale ϵ in our calculations as time proceeds.

Case III: Stable-unstable-stable atmosphere

In Fig. 11, we show the mean velocity at 3000 sec for the production of a shear layer in a stable-unstable-stable atmosphere. Note again that this is not much changed from the two previous cases although there has been slightly more diffusion of the mean velocity profile.

In Fig. 12, we again see a marked effect of the mean-temperature profile on the turbulence production. In this case, the thermal instability at small times produces a great deal of turbulence in the unstable layer trapped between two stable layers. Only towards the maximum of the mean motion does the shear-produced turbulence make its presence felt.

Figure 13 is a plot of the behavior of $\overline{w'T'}$ and l. Here we see again that very large turbulent heat fluxes are developed in the unstable region $\partial T/\partial z < 0$, while it has been virtually impossible to produce any heat flux in the region where $\partial T/\partial z > 0$. This is another example of the difficulty of getting rid of inver-

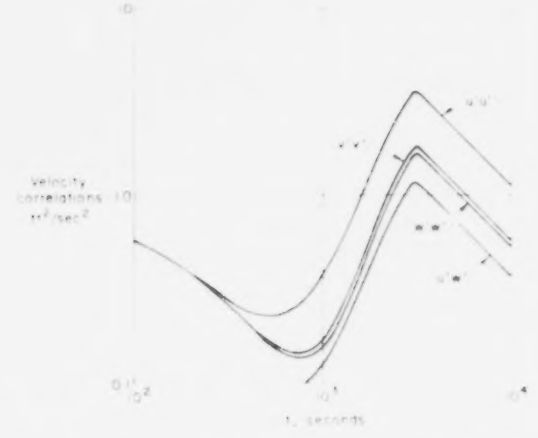

Fig. 6. Maxima of velocity correlations: Case I.

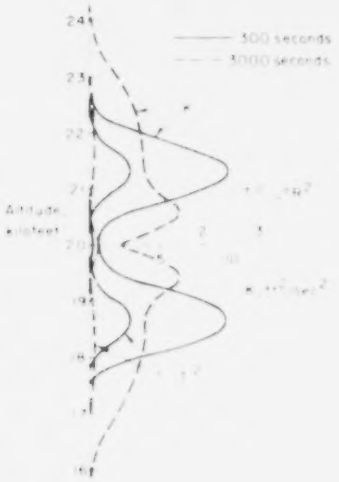

Fig. 8. l and K for Case II at 3000 sec.

59

Fig. 9. T and $w'T'$ for Case II at 300 and 3000 sec.

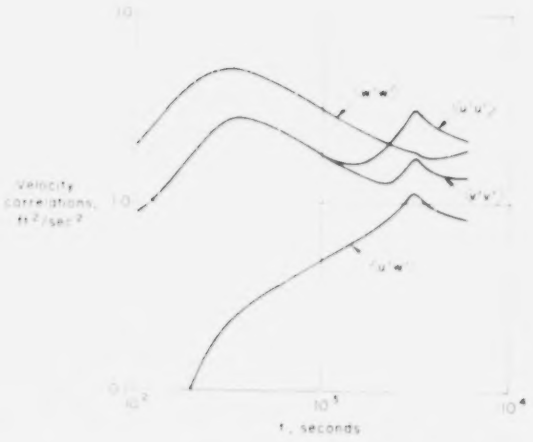

Fig. 10. Maxima of velocity correlations; Case II.

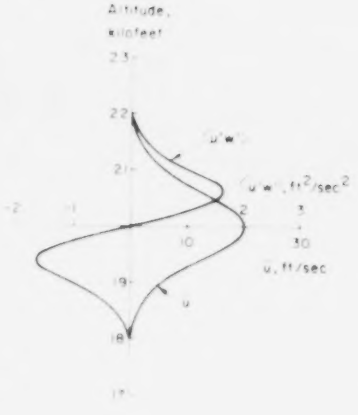

Fig. 11. u and $u'w'$ for Case III at 3000 sec.

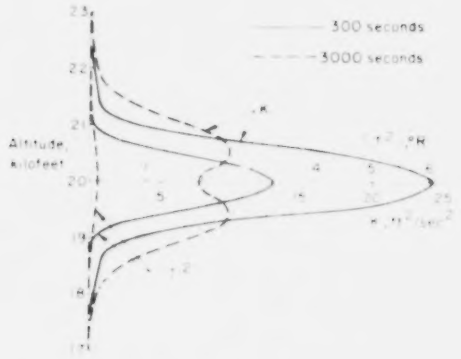

Fig. 12. T and K for Case III at 300 and 3000 sec.

sions. Again this reluctance of nature to establish a heat flux when $\partial T/\partial z > 0$ is a basic characteristic of the atmosphere and cannot be described by any simple eddy-diffusivity model.

In Fig. 14 we show the behavior of the maxima of the velocity correlations as a function of time for this case of shear-layer formation. Note that the effect of shear-generated turbulence makes itself evident only when the mean flow is near its maximum velocity.

Case IV: Stable-unstable atmosphere

In Fig. 15, we have plotted the mean-velocity profile and the profile of $w'w'$ for a time of 3000 sec. Here we again note the similarity of this profile to all the previous cases.

In Fig. 16, we show the behavior of T^2 and K for $t = 3000$ sec. In this case we note that there are two extrema of K. Both are close to the point where $\partial T/\partial z$ is a maximum, as might be expected. The production of turbulent energy on the unstable side exceeds that on the stable side but not by as much as we had expected prior to making these calculations.

In contrast to the behavior of the turbulent energy, we see from Fig. 17 that the production of $w'T'$ is vastly different in the stable and in the unstable regions. We note again that it is extremely difficult to produce any $w'T'$ in a stable region, so that the temperature inversion in $\partial T/\partial z > 0$ is extremely persistent. Again, no presently used eddy-diffusivity model would predict the result we have shown.

In Fig. 18, we show the behavior of the maxima of the velocity correlations as a function of time. We note again the initial production of turbulence by means of thermal instability, the modification of this by the action of shear-generated turbulence near the time of maximum mean velocity, and the final phase of the motion when the production of turbulence by

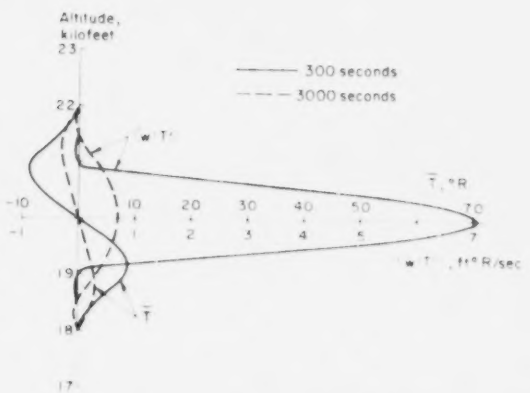

Fig. 13. T and $w'T'$ for Case III at 300 and 3000 sec.

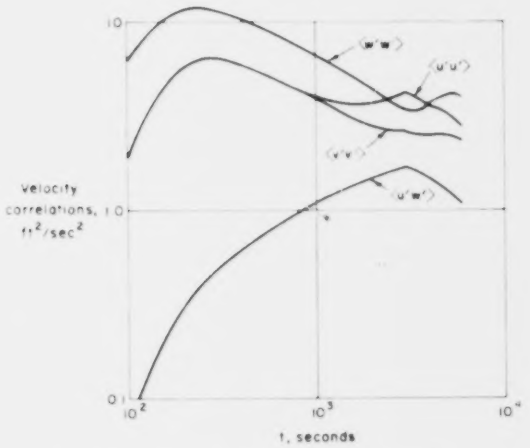

Fig. 14 Maxima of velocity correlations; Case III.

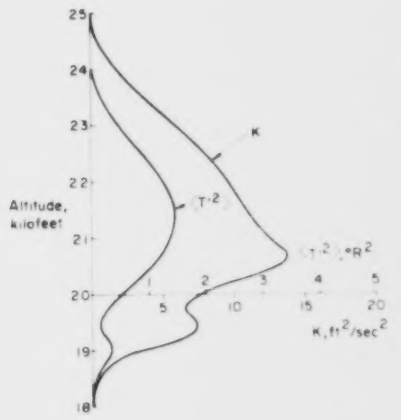

Fig. 16 $\langle T^2 \rangle$ and K for Case IV at 3000 sec.

thermal instability in the decaying thermal layer is just about balanced by dissipation so that a rather constant level of turbulent energy results.

Discussion of Results

The most interesting aspect of the results we have just presented is the radically different behavior of the heat flux correlation $\langle w'T' \rangle$ depending on whether $\partial T/\partial z$ is greater or less than zero. The explanation for this behavior lies in the equations and may be exhibited as follows.

Consider a flow in which there is no mean motion and in which all quantities except T are independent of z. In this case, the pertinent equations for the production of correlations obtained from Eqs. 54, 57, and 58 are

$$\frac{\partial \langle w'w' \rangle}{\partial t} = \frac{2g}{T_0}\langle w'T' \rangle - \frac{q}{\Lambda}\left(\langle w'w' \rangle - \frac{K}{3}\right) - \frac{2\mu}{\rho_0}\frac{\langle w'w' \rangle}{z^2} \tag{67}$$

$$\frac{\partial \langle w'T' \rangle}{\partial t} = -\langle w'w' \rangle \frac{\partial T}{\partial z} + \frac{g}{T_0}\langle T^2 \rangle - \frac{q}{\Lambda}\langle w'T' \rangle - \frac{2\mu}{\rho_0}\langle w'T' \rangle \tag{68}$$

$$\frac{\partial \langle T^2 \rangle}{\partial t} = -2\langle w'T' \rangle \frac{\partial T}{\partial z} - \frac{2\mu}{\rho_0}\frac{\langle T^2 \rangle}{z^2} \tag{69}$$

If we consider only the production terms and neglect the tendency-towards-isotropy terms and dissipation terms in these equations, we have

$$\partial \langle w'w' \rangle / \partial t = (2g/T_0)\langle w'T' \rangle \tag{70}$$

$$\partial \langle w'T' \rangle / \partial t = -\langle w'w' \rangle \partial T/\partial z + (g/T_0)\langle T^2 \rangle \tag{71}$$

$$\partial \langle T^2 \rangle / \partial t = -2\langle w'T' \rangle \partial T/\partial z \tag{72}$$

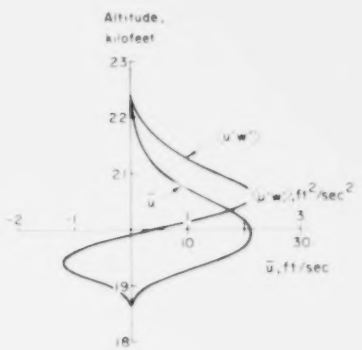

Fig. 15 $\bar{u}$ and $\langle u'w' \rangle$ for Case IV at 3000 sec.

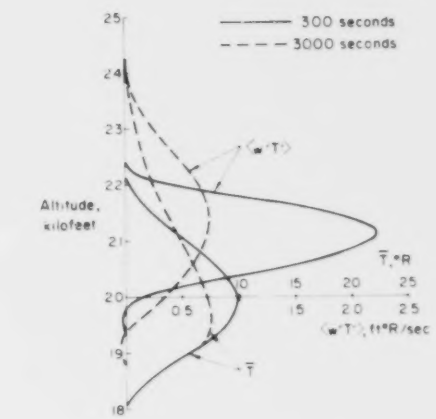

Fig. 17 $\bar{T}$ and $\langle w'T' \rangle$ for Case IV at 300 and 3000 sec.

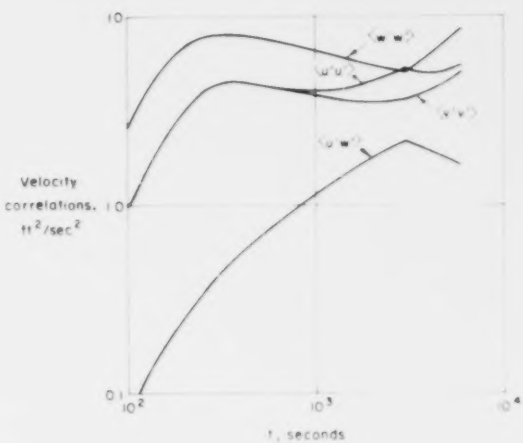

Fig. 18 Maxima of velocity correlations; Case IV.

We now assume (on the basis of experience with existing calculations) that the rate of change of $\partial T/\partial z$ is very slow compared to the rate of change of the second-order correlation. In this case we can assume, to first order, that $\partial T/\partial z$ is a constant and eliminate $\langle w^2 \rangle$ and $\langle T^2 \rangle$ from Eq. (71) by differentiating that equation with respect to time and using Eqs. (70) and (72). The result is

$$\frac{\partial^2 \langle wT \rangle}{\partial t^2} = -(4g^2 T_0^2 \beta^2 \partial T/\partial z)\langle wT \rangle \tag{73}$$

Examination of this equation shows that when $\partial T/\partial z < 0$, there is an exponential development of $\langle wT \rangle$. However, when the atmosphere is stable, i.e., $\partial T/\partial z > 0$, the heat-flux correlation $\langle wT \rangle$ is oscillatory with frequency

$$\omega = 2[(g^2 T_0^2 \beta^2 \partial T/\partial z)]^{1/2} \tag{74}$$

In fact the general solution for Eqs. (70–72) may be written

$$\langle wT \rangle = A \sin \omega t + B \cos \omega t \tag{75}$$

$$\langle ww \rangle = [\omega/(2\beta^2 T_0^2 g)][-A \cos \omega t + B \sin \omega t] + C \tag{76}$$

$$\langle T^2 \rangle = (2\beta/\omega T_0 g)[A \cos \omega t - B \sin \omega t] + (1/g\beta^2 T_0^2) \tag{77}$$

When the general case in which both the tendency-towards-isotropy terms and dissipation are considered, i.e., Eqs. (67–69), there results a damped oscillation of the quantities $\langle wT \rangle$, $\langle ww \rangle$, and $\langle T^2 \rangle$. In fact, if Λ is sufficiently large compared to ε so that only dissipation need be considered, the solution becomes $\exp[-2at(\mu_0 \varepsilon^2)]$ times each of the expressions given above.

A close examination of all our numerical results shows this oscillatory behavior at the frequency given above during the early phases of each run in the region where $\partial T/\partial z > 0$.

The upshot of all this discussion is that the basic equations of atmospheric motion indicate a vast difference between the behavior of $\langle wT \rangle$ when $\partial T/\partial z < 0$ and when $\partial T/\partial z > 0$. In the unstable case, a large heat flux is established quite rapidly. In the stable case, the heat flux tends to oscillate about a value that is very small. This results in an extraordinary persistence for temperature inversions in the atmosphere. It also means that the idea of a simple eddy diffusivity in the atmosphere is completely wrong and will, when used in calculations, result in far too rapid a dissipation of any inversions.

Conclusions and Recommendations

We have presented the first results using the method of invariant modeling to calculate the behavior of atmospheric shear layers. We realize we have only scratched the surface; much remains to be done. In particular, we are working towards a better method for putting the scale length Λ into our equations. We would eventually like to have an explicit equation for Λ which could be carried along as an extra simultaneous equation to be solved. For certain cases, namely, the production of thermal turbulence, this is probably more important than in the case of shear-driven turbulence. In this connection, mention should be made of the recent work of Harlow et al.[9,10] which is closely related to our own studies.

Although the authors recognize that much still needs to be done to finalize a general method for predicting wind-driven atmospheric motion, we feel that the method of invariant modeling represents a powerful basic tool with which to approach this problem. It seems clear from our studies to date that the eddy-diffusivity concept should be discarded as a means by which the gas dynamicist attacks the problem of turbulent motions in the atmosphere.

In regard to future applications of the method we have just presented, it should be mentioned that equations similar to those considered here can be written for correlations of fluctuations in species concentration. Thus, application of this method to the convection and diffusion of gaseous pollutants in the atmosphere is straightforward. In particular, the effect of a stable lapse rate on the development of turbulent mass transport is similar to that found for the turbulent transport of heat in this study.

References

[1] Donaldson, C. duP., "A Computer Study of an Analytical Model of Boundary Layer Transition," *AIAA Journal*, Vol. 7, No. 2, Feb. 1969, pp. 271–278.

[2] Donaldson, C. duP. and Rosenbaum, H., "Calculation of Turbulent Shear Flows Through Closure of the Reynolds Equations by Invariant Modeling," Rept. 127, Dec. 1968, Aeronautical Research Associates of Princeton Inc., Princeton, N.J.

[3] Prandtl, L., "The Mechanics of Viscous Fluids," *Aerodynamic Theory*, Vol. III, edited by W. F. Durand, Dover Publications, New York, 1963.

[4] Glushko, G. S., "Turbulent Boundary Layer on a Flat Plate in an Incompressible Fluid," *Bulletin of the Academy of Sciences of the USSR*, Mechanical Series, No. 4, 1965.

[5] Beckwith, I. E. and Bushnell, D. M., "Detailed Description and Results of a Method for Computing Mean and Fluctuating Quantities in Turbulent Boundary Layers," TN D-4815, 1968, NASA.

[6] Coles, D. E. and Hirst, E. A., editors, *Proceedings—Computation of Turbulent Boundary Layers*, AFOSR-IFP-Stanford Conference, Vol. II, Aug. 18–25, 1968.

[7] Lumley, J. L. and Panofsky, H. A., *The Structure of Atmospheric Turbulence*, Interscience Publishers, New York, 1964.

[8] Harlow, F. H. and Nakayama, P. I., "Turbulence Transport Equations," *The Physics of Fluids*, Vol. 10, No. 11, 1967.

[9] Harlow, F. H. and Romero, N. C., "Turbulence Distortion in a Nonuniform Tunnel," Rept. LA-4247, 1969, Los Alamos Scientific Lab., Los Alamos, N. Mex.